NAVAL POSTGRADUATE SCHOOL
Monterey, California

THESIS

HUMAN-POWERED HELICOPTER:
A PROGRAM FOR
DESIGN AND CONSTRUCTION

by

Scott Alan Bruce

June, 1991

Thesis Advisor: E. Roberts Wood

Approved for public release; distribution is unlimited.

T256897

UNCLASSIFIED
RITY CLASSIFICATION OF THIS PAGE

REPORT DOCUMENTATION PAGE

Form Approved
OMB No 0704-0188

REPORT SECURITY CLASSIFICATION Unclassified	1b RESTRICTIVE MARKINGS
ECURITY CLASSIFICATION AUTHORITY	3 DISTRIBUTION/AVAILABILITY OF REPORT
DECLASSIFICATION/DOWNGRADING SCHEDULE	
RFORMING ORGANIZATION REPORT NUMBER(S)	5 MONITORING ORGANIZATION REPORT NUMBER(S)
NAME OF PERFORMING ORGANIZATION val Postgraduate School 6b OFFICE SYMBOL (If applicable) 31	7a NAME OF MONITORING ORGANIZATION Naval Postgraduate School
ADDRESS (City, State, and ZIP Code) nterey, CA 93943-5000	7b ADDRESS (City, State, and ZIP Code) Monterey, CA 93943-5000
NAME OF FUNDING/SPONSORING ORGANIZATION 8b OFFICE SYMBOL (If applicable)	9 PROCUREMENT INSTRUMENT IDENTIFICATION NUMBER
ADDRESS (City, State, and ZIP Code)	10 SOURCE OF FUNDING NUMBERS PROGRAM ELEMENT NO / PROJECT NO / TASK NO / WORK UNIT ACCESSION NO

TITLE (Include Security Classification) Human Powered Helicopter: A program for Design and ntruction

PERSONAL AUTHOR(S)
Bruce, Scott A.

TYPE OF REPORT	13b TIME COVERED	14 DATE OF REPORT (Year, Month, Day)	15 PAGE COUNT
ster's Thesis	FROM _____ TO _____	June 1991	131

SUPPLEMENTARY NOTATION The views expressed in this thesis are those of the thor and do not reflect the official policy or position of the Dept. of fense or the U.S. Government.

COSATI CODES		
FIELD	GROUP	SUB-GROUP

18 SUBJECT TERMS (Continue on reverse if necessary and identify by block number)
Human-Powered Helicopter
Helicopter
Human Power

ABSTRACT (Continue on reverse if necessary and identify by block number)

The various aspects of helicopter design and human-powered aircraft design are studied to present a program to design and build a human-powered helicopter (HPH) at the Naval Postgraduate School. The HPH will be designed to meet the requirements for the AHS-Sikorsky Award . The helicopter design is refined, and the feasibility of construction is assessed. In addition to pursuing a significant historical achievement, the program seeks to enhance the helicopter and composite programs of the Aeronautical Engineering curriculum at the NPS. Benefits to NPS in terms of research topics and as a research aircraft are presented. Potential future uses for ultra-low powered aircraft technology are also outlined.

DISTRIBUTION/AVAILABILITY OF ABSTRACT ☒ UNCLASSIFIED/UNLIMITED ☐ SAME AS RPT ☐ DTIC USERS	21 ABSTRACT SECURITY CLASSIFICATION Unclassified
NAME OF RESPONSIBLE INDIVIDUAL .W. Wood	22b TELEPHONE (Include Area Code) 408 646-2311 22c OFFICE SYMBOL AA/Ew

Form 1473, JUN 86 *Previous editions are obsolete*
S/N 0102-LF-014-6603

SECURITY CLASSIFICATION OF THIS PAGE
UNCLASSIFIED

Approved for public release; distribution is unlimited.

HUMAN-POWERED HELICOPTER: A PROGRAM FOR DESIGN AND CONSTRUCTION

by

Scott A. Bruce
Lieutenant Commander, United States Navy
B.S., United States Naval Academy, 1979

Submitted in partial fulfillment
of the requirements for the degree of

MASTER OF SCIENCE IN AERONAUTICAL ENGINEERING

from the

NAVAL POSTGRADUATE SCHOOL
June, 1991

Department of Aeronautics and Astronautics

ABSTRACT

The various aspects of helicopter design and human-powered aircraft design were studied to present a program to build a human-powered helicopter (HPH) at the Naval Postgraduate School. The HPH will be designed to meet the requirements for the AHS-Sikorsky Award. The helicopter design is refined, and the feasibility of construction is assessed. In addition to pursuing a significant historical achievement, the program seeks to enchance the helicopter and composite programs of the Aeronautical Engineering curriculum at the NPS. The benefits to NPS in terms of research topics and a research aircraft are presented. Potential future uses for ultra-low-powered aircraft technology are also outlined.

C.1

TABLE OF CONTENTS

I. INTRODUCTION TO HUMAN-POWERED FLIGHT 1

A. HISTORY OF HUMAN-POWERED FLIGHT 1

1. Fixed Wing 1

2. Rotary Wing 3

B. IGOR I. SIKORSKY HUMAN-POWERED HELICOPTER COMPETITION 3

C. POTENTIAL USES FOR ULTRA-LOW-POWERED AIRCRAFT . 4

II. DESIGN BACKGROUND 6

A. POWER AVAILABLE 6

1. Pilot Position 6

2. Past Studies 7

3. Power Versus Time 11

4. Miner's Rule Applied to Human Power Levels . 12

5. Ergometer 15

B. LESSONS LEARNED FROM PAST HUMAN-POWERED AIRCRAFT 16

III. AIRCRAFT DESIGN 20

A. HUMAN-POWERED AIRCRAFT DESIGN THEORY 20

B. ROTOR CONFIGURATION 22

C. AIRFOIL SELECTION 23

1. Preliminary Considerations 23
2. Airfoil Selection Criteria 23
3. Low Reynolds Number Airfoil Design Theory . 25
a. Reynolds Number Defined 25
b. Drag 26
c. Separation Bubble 27
d. Stall Hysteresis 27
e. Wind Tunnel Testing 28
f. Turbulence 29
g. Summary. 30
4. Final Airfoil Selection 31
D. PLANFORM 35
1. Preliminary considerations 35
2. Rotor Diameter 36
3. Twist and Taper 37
4. Tip losses 42

IV. PERFORMANCE 44
A. HOVER PERFORMANCE 44
1. Hover power calculations 44
2. Vortex lattice method 47
3. Approximation accuracy 48
a. Pitch angle equal to the angle of attack 48
b. Inflow on the lower set of rotor blades 50
B. GROUND EFFECT 53
1. Theory 53

2. Ground Effect Calculations 56
a. 3-meter height 56
b. Deep In Ground Effect 57
c. Summary of Ground Effect Calculations . 57
C. STABILITY AND CONTROL 58
1. Controllability 59
2. Static Stability 60
3. Lateral and Longitudinal Control 62
4. Directional Control 63
5. Collective Control 64
6. Energy Storage 64

V. FINAL CONFIGURATION 65
A. CONSTRUCTION 67
B. MAIN SPAR DESIGN 68
1. Composite Technology Background 68
2. Composite Tube Construction 70
3. Composite Material Selection 70
4. Bending to Torsion Coupling 71
C. ROTOR BLADES 72
D. DRIVE TRAIN 74
1. Chain/crank system 74
2. Reversing Mechanism 76
E. SUMMARY OF FINAL DESIGN 77

VI. CONCLUSIONS AND RECOMMENDATIONS 79
A. BENEFITS OF AN HPH PROGRAM 79
B. FLIGHT TEST OPPORTUNITIES 81
1. Highly flexible aircraft 81
2. Instrumentation research 82
3. Flying Qualities 82
4. Simulation 82
C. AREAS FOR FUTURE RESEARCH 83
1. Low Reynolds number design and test 83
2. Flexible airfoil design and test 83
3. Deep in ground effect hover theory 83
4. Tip losses for low induced velocity rotors/wings 83
D. FOLLOW-ON WORK 84
1. Main rotor spar 85
2. Main mast and reversing mechanism 85
3. Ergometer 85
4. Main rotor blades 85
5. Undercarriage 86
6. Flight control system 86
7. Construction of a simulator 86
E. SUMMARY 86
REFERENCES 90
APPENDIX A: FIGURES. 94
APPENDIX B: TABLES 99
APPENDIX C: HPH COMPETITION RULES. 101

APPENDIX D: ERGOMETER. 106
APPENDIX E: FORCE TRANSDUCER 107
APPENDIX F: COMPUTER PROGRAMS. 109
APPENDIX G: MYLAR INFORMATION. 116
APPENDIX H: HPH DRAWINGS 117
INITIAL DISTRIBUTION LIST. 120

ACKNOWLEDGEMENT

I wish to acknowledge several people, without whom this project would never have begun. The support of Prof. Rick Howard was instrumental in understandiong low-Reynolds-number airfoil theory. The technical and moral support of Mr. Peter Zwann provided insight only available from someone who has attempted a project such as this. I especially wish to thank Prof. Bob Wood for allowing me the freedom to pursue my dream. His vast understanding of helicopters was invaluable, and he always seemed to provide just the right amount of guidance and encouragement when it was needed. Finally, without the personal sacrifices, love, and support on the part of my wife, Lauri, and children, Amie and Nicholas, I couldn't have finished my portion of this immense undertaking.

I. INTRODUCTION TO HUMAN-POWERED FLIGHT

A. HISTORY OF HUMAN-POWERED FLIGHT

1. Fixed Wing

The development of modern human-powered aircraft technology has been motivated primarily by a series of prizes. The first significant step toward building a human- powered aircraft capable of level flight occurred in 1935 when an aircraft called the Mufli competed for a 5,000 Mark prize. Although unable to sustain level flight, it none-the-less represented the first serious attempt to achieve human-powered flight.[Ref.1: p.141]

In 1959 a British industrialist named Henry Kremer offered a prize of 5,000 pounds sterling for the first human-powered aircraft to fly a figure-eight course around two pylons one-half of a mile apart. Although aircraft had been able to fly a straight mile for many years it was not until 1977 that the problem of making the turns was solved. The Gossamer Condor, designed by Dr. Paul MacCready Jr., won the prize which had increased to 50,000 pounds by then.

It was MacCready's innovative thinking in attacking the overall problem that allowed the team to win the prize. MacCready designed a lightweight and simple airframe with a much larger planform (95-foot span with a 12-foot chord) than

most of the human-powered aircraft flying at the time. A larger planform allowed the airspeed to be slowed down to 10mph--well below the airspeed of any human-powered aircraft that had been flying at the time. The highly flexible aircraft then had a problem during turns. As a conventional-type aileron was deflected in order to generate higher lift on one wing, the wing would just twist. The Gossamer team was unable to generate sufficient roll moment to turn, so they used a canard wing that could be tilted with respect to the aircraft longitudinal axis to generate a yaw moment. The yaw motion generated an airspeed differential on the two wings which in turned rolled the aircraft in the direction of the yaw. With the introduction of roll-yaw aerodynamic coupling for turns and the very low airspeed to reduce the power required, they were easily able to win the first Kremer Prize. [Ref.2: Chap.4]

In 1979, the same team won a 100,000-pound prize offered by Kremer for flying across the English Channel. In doing so the team also increased the distance record for human- powered aircraft to 21 miles.[Ref.1: p.141]

Perhaps the most notable achievement in human-powered flight to date has been a venture called the Daedalus Project. A team originating from MIT built an aircraft to re-create the mythical flight by Daedalus from Crete to an island 72 miles away. The team took several years and spent nearly a million dollars, used the highest technological materials and

methods, and created an aircraft with a wingspan larger than most airliners but weighing only 68 pounds. In the process of achieving their goal, they built a prototype airplane called the Light Eagle. The Light Eagle was used to conduct many flight tests at Edwards AFB, and set many records in the process, including extending the distance record to over 37 miles.[Ref.4]

2. Rotary Wing

The effort to build a human-powered helicopter has not been as successful as the fixed-wing efforts. Although many have been built in the U.S., U.K., Germany and Japan, the only helicopter to achieve flight has been an aircraft called the Da Vinci III. The Da Vinci III is a single-piloted, two-bladed, single-main-rotor, tip-driven helicopter with a 100-ft radius. Inspired by the Igor I. Sikorsky Human-powered Helicopter Competition (see next section), the Da Vinci finally achieved the first human-powered hover in Dec, 1989. Built by engineering students at California Polytechnic University, San Luis Obispo, it represented the third aircraft they have built in a program that started in 1981. [Ref.3: p.30]

B. IGOR I. SIKORSKY HUMAN-POWERED HELICOPTER COMPETITION

In 1980 the American Helicopter Society offered a prize of $10,000 to the first human-powered helicopter and established a set of rules to govern the competition. As of May 1991, the

prize money stood at $20,000. The basic requirements of the Igor I. Sikorsky Award are that:

- The helicopter must hover for one minute.
- The helicopter must momentarily achieve a height of three meters.
- The helicopter must remain within a square that is ten meters on each side.
- As many pilots as desired may be used.
- No forms of energy storage may be used.
- The pilot(s) must not rotate.

A complete copy of the competition rules is included as Appendix C.

C. POTENTIAL USES FOR ULTRA-LOW-POWERED AIRCRAFT

Before discussion of the aircraft design, a quick look at some of the practical applications of ultra-low-powered flight technology is given. This section is meant to show the reader that this project is not merely a sensational attempt to earn a spot in the history books, but that there are serious benefits to be realized from the project. Benefits as a research vehicle and test aircraft, in addition to the research subjects necessary to complete the project, are presented in Chapter VI.

Aircraft which require very little power include very long endurance aircraft. In this respect, human-powered aircraft technology would be suitable for reconnaissance, surveillance,

and search aircraft; much in the same vein that lighter-than-air aircraft are under consideration for the same missions. Very high altitude aircraft also operate in the low Reynolds number flight regime, despite having a relatively high Mach number.

A practical and safe vertical takeoff and landing Remotely Piloted Vehicle (RPV) design is needed for shipboard application. Use of this ultra low powered technology would allow a large payload and have tremendous endurance. It would also have the advantage of being fabricated with inexpensive materials, rendering the aircraft expendable. The slow rotation of the blades make for a much safer vehicle, especially in the cramped shipboard application.

Another possible by-product might be an aircrew escape system. If a parafoil could be made to have a lift-to-drag ratio of 30, a pilot ejecting at 12,000 feet could glide 60 miles to a safe area.

Although a helicopter powered by one person will not specifically have any direct application to aviation in general, the technology derived from a project such as this can be used to develop future aviation-related projects.

II. DESIGN BACKGROUND

A. POWER AVAILABLE

1. Pilot Position

Most non-flight-vehicle related human-powered references and studies refer to a "rider" as the person who controls and provides the power to propel a human-powered vehicle. Since our vehicle is a helicopter, the operator for this aircraft will hereafter be referred to as the "pilot".

Human-powered vehicles in general have the riders in one of three positions: upright, prone recumbent (stomach down, head forward), and supine recumbent (stomach up, head to the rear). The upright position has an advantage by being the most familiar, as it is the position for a conventional bicycle. Studies have shown that the recumbent position delivers more power, but has the disadvantage of requiring time to adapt. A rider requires approximately a one-month adaption period to become fully accustomed to a novel bicycle.[Ref.5: p.30]

The recumbent position also has the advantage of being the most compact with respect to the vertical axis. This will be important in making the aircraft as low as possible. By keeping the Center of Gravity low, the aircraft will be less

prone to rollover. Most importantly, it will keep the blades as low as possible to take maximum advantage of ground effect.

The supine recumbent position represents the most comfortable and practical of the two supine positions. In the supine recumbent position, the body is doubled over more than the prone recumbent position with the weight of the head supported by the spine. Hence, it is a more natural and relaxed position. The support necessary for the supine recumbent position is less complicated, easier to design and build, and will be lighter than the support for the prone recumbent position. As such the supine recumbent position (laying down, feet forward) will be the position of choice for this design.

2. Past Studies

There have been exhaustive studies on human power output, studying everything from the various physical dimensions to nutrition studies to body size and composition. In performing any physiological study there are literally an infinite number of variables involved, and it becomes a study in minimizing the impact of the uncontrollable variables with respect to the variables being measured. As a result, there is a large amount of data scatter and even conflicting results. Thus, the best that can usually be gleaned from the studies is a good "feel" for trends and the magnitude of effects of the variables associated with human power output.

A review of past human power output studies is necessary to estimate power levels and to design the position and associated equipment for maximum power output. Conventional bicycle cranks, pedals and chainwheels provide a proven system which is reliable and simple and will be used for this design. Although studies have shown that up to 18% more power can be generated by combined hand cranking and pedalling [Ref.5: p.44], that combination will be impractical for this design. The pilot will be required to use his hands to control the aircraft, and the added power will be negated by the added weight of the necessary mechanism.

To determine the necessary gearing for the drive train and transmission, the optimum pedal speed must be determined first. The following pedalling parameters that can be varied to achieve the highest power for one minute are to be considered:

- Pedalling RPM
- Saddle height
- Crank length
- Chainwheel ellipticity

It has been shown that although the most efficient pedalling rate is approximately 60 rpm, the most power can be put out at the highest rpm attainable.[Ref.5: p.49] The reason for this is that muscle cells cannot exert a continous force but contract in extremely rapid spasms much like a piston

"firing". Thus, the individual cells can exert a proportionately larger force when the muscle bundle is not required to produce a long slow contraction but a quick powerful one.

During bicycle races, riders will often exceed 200 rpm during sprints. In achieving such high pedalling rpms there is often a great deal of relative motion between the rider and the cycle which would render such high rpms impractical for a design of this nature. Figure 1 shows the relationship between power, efficiency and torque for pedalling rpm. In achieving higher pedalling rpms, pedalling technique becomes the overriding factor in determining the maximum power output.

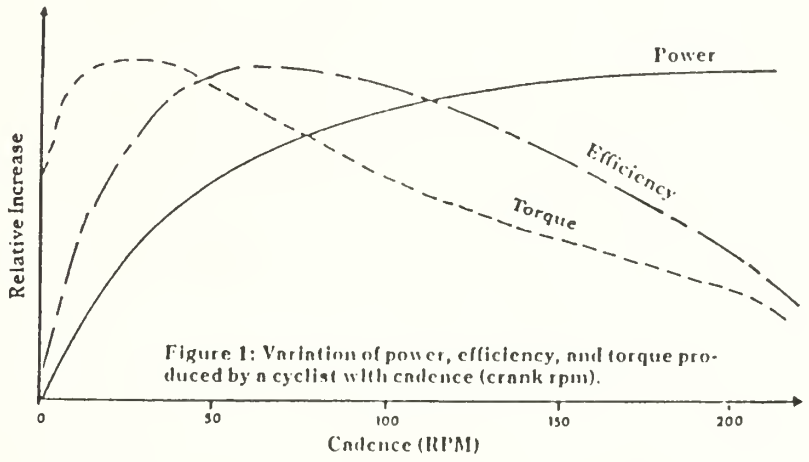

Figure 1: Variation of power, efficiency, and torque produced by a cyclist with cadence (crank rpm).

Figure 1. VARIATION OF POWER, EFFICIENCY, AND TORQUE PRODUCED BY A CYCLIST WITH CADENCE (CRANK RPM). [REF.6: P.10]

Recent ergometer tests on the Italian National Sprinting team have shown that for short durations (five to ten seconds)

maximum power was achieved at about 120 rpm. Over the course of several minutes, 60 to 80 rpm gave the maximum power.[Ref.7: p.7]

Thus, there is no single, ideal rpm that will give the highest power over one minute, as the exact relation between efficiency and speed cannot be explicitly determined. However, as an estimate based on the previously mentioned studies and the racing experience of the author, the aircraft should be geared for 90 rpm. The use of standard bicycling components will allow the pedals, chainwheel and cranks to be easily changed to suit individual pilot technique and experience. Additionally, the use of easily- interchangeable standard components will allow simple adjustment of the main-rotor-drive-system gear ratio.

A saddle height 1.8 to 2.0 inches above the height where the heel can just touch the pedal at the bottom of the stroke has been shown to give the most power.[Ref.5: p.53] This will correspond to a slightly longer seatback-to-crank- hub length, and will need to be taken into account when testing for pilots and adjusting the aircraft.

Crank length has not been extensively tested since most human-powered studies are for conventionally-pedalled bicycles and the crank length is usually limited by bicycle/ground clearance. Consequently, the range of crank lengths available for conventional bicycles falls into a very narrow range due to safety considerations. Crank length is typically 165-170mm

for conventional bicycles. Studies seem to indicate that more power can be achieved for limited periods of time with cranks five to ten percent longer, but the results are not conclusive.[Ref.5: p.53] Pilot technique and familiarity will probably necessitate the use of standard lengths, although tests need to be conducted to find the optimum length for the particular situation.

The use of elliptical chainwheels is a controversial subject. Studies have shown that a high degree of ovality (on the order of 1.2:1 and greater) definitely decreases performance. However, moderately elliptical chainwheels of the order of 1.1:1 seem to often improve performance but never diminish performance. [Ref.5: p 56]

3. Power Versus Time

Figure 2 presents human power output for various times. The data scatter demonstrates the difficulty in precisely defining the variables and parameters necessary for a physiological application such as this. As such, it becomes necessary to use one's best judgement and intuition in applying these data to the aircraft design.

There are a number of top-quality bicycle racers locally. The HPH team will have access to "well-trained and highly-conditioned" athletes, so it would be reasonable to expect up to 1.5 hp for several seconds from such a pilot. Therefore, 1.5 hp will be used as the upper limit of power for the 3-

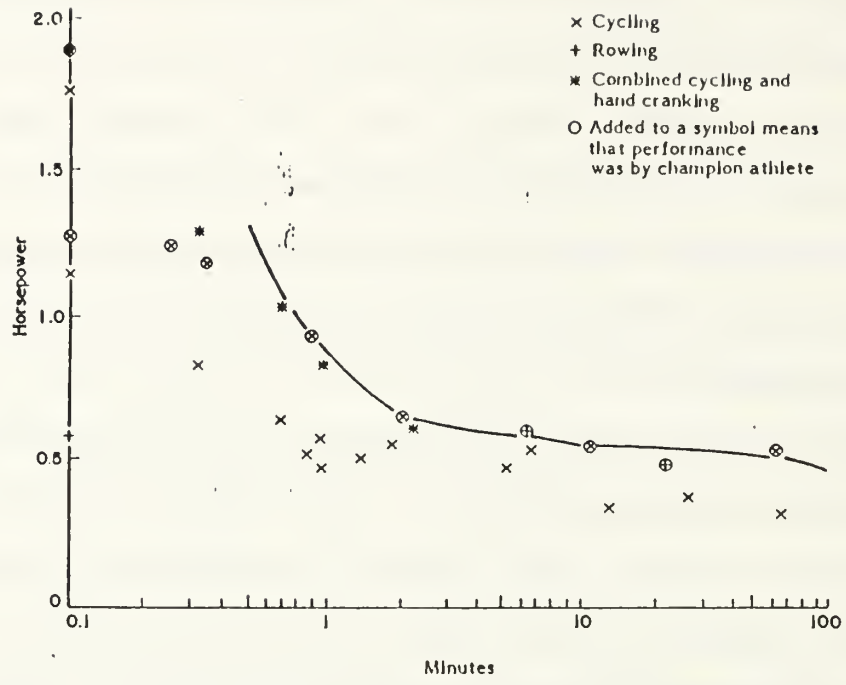

Figure 2. HUMAN POWER OUTPUT VERSUS TIME [REF.2: P.4-2]

meter hover condition, which corresponds to the condition with the highest power requirement.

4. Miner's Rule Applied to Human Power Levels

Studies in human power output all hold the power constant until exhaustion is reached. In this application, two power levels will be needed over the course of one minute: one at the 3 meter height which will be required for approximately 5 seconds, and one very deep in ground effect. Thus, a method determining the power available at *two* levels over the course of one minute is needed.

Miner's rule is a simple method often used to calculate cumulative fatigue damage for mechanical elements. The rule is applied to a component which undergoes non-constant cyclic

stress where the number of cycles is known at each different stress level. Miner's rule calculates the life of an component based on the percentage of the life used at each stress level. When the sum of the percentages at each stress level reaches 100%, the component has reached its fatigue life.

Mathematically, Miner's rule is stated as:

$$\frac{n_1}{N_1} + \frac{n_2}{N_2} + \ldots = 1 \qquad (1)$$

where: n_x = the number of cycles at stress x

N_x = the number of cycles to to the fatigue life at stress level x

A typical S-N curve is presented in Figure 3. The horizontal axis represents the number of cycles and is often a logarithmic scale, and the vertical axis is the stress level. The resemblance of this curve to a human power versus time curve can be seen by comparing this curve to that in Figure 2.

In applying Miner's Rule to human power, the power level is substituted for stress level and time is substituted for the number of cycles. The pilot will be required to put out a higher power level for approximately 5 seconds, and a lower power level for 55 seconds. The equation becomes:

$$\frac{5}{Tp_1} + \frac{55}{Tp_2} = 1 \qquad (2)$$

where: Tp_1 = the time at power level 1

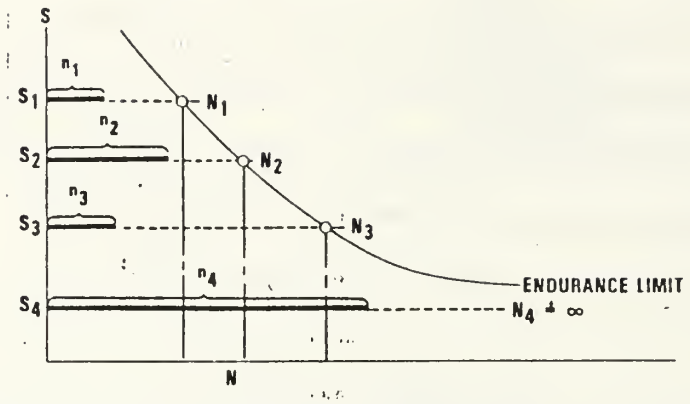

Figure 3. TYPICAL STRUCTURAL COMPONENT S-N CURVE [REF.8: P.2-6]

Tp_2 = the time at power level 2

The analogy appears justified upon examining the physiological mechanism behind working the human muscle to exhaustion. The energy created by a muscle is created by the breakdown of ATP (adrenosine triphosphate) within the muscle cells. The cell uses glycogen to break down the ATP, and the glycogen is created by oxidizing glucose and fatty acids with oxygen supplied from the blood. There is a small amount of glycogen stored within the muscle tissue for immediate use, but extended exercise requires a steady supply of glucose or fat from the blood system.

Thus, there are two primary modes in which the muscle functions. The first is the "aerobic" mode where the energy demanded by the muscle can be offset by oxygen from the blood. In the "anaerobic" mode, the muscle can provide limited power by relying on stored energy. The time a muscle can continue to

function anaerobically depends on the power output demanded and lasts anywhere from 30 seconds to several minutes.

The shape of the human power versus time curve is governed by these two modes of performance. For short periods the muscle functions on stored reserves, and the power is governed by maximum strength. As the period of time increases, the muscle increasingly relies on the blood to supply oxygen to burn stored glycogen and the power decreases to a point where the blood can supply both the oxygen and the oxidants necessary to sustain the performance for several hours. This sustained power level then equates to the endurance limit for mechanical components.

The muscle reaches exhaustion and ceases to function when the stored energy supplies are depleted, or are used up faster then the blood can replenish them. Thus, Miner's Rule would apply, where the "life" of the muscles is that point where the stored glycogen is depleted or the rate that stored and blood-supplied energy is exceeded. Just as a mechanical component fails at the fatigue life, when the muscle reaches exhaustion it ceases to function as well.

5. Ergometer

An ergometer is an apparatus designed to measure the amount of work done by a human. Construction of an ergometer was begun, but not completed. A photograph of the ergometer is included in Appendix D. The purpose of the ergometer is

manifold. Anthropometric data are needed to determine the dimensions for the pilot support structure, called the "undercarriage." Pilot power measurements will be the most valuable data to be determined. In concert with power measurements is testing the various parameters involved with pedal power e.g., crank length, elliptic chainwheels, pedal speed, etc. The ergometer will be instrumental in aiding to select the pilot. Once selected, the pilot will need a one-month adjustment period to be able to achieve maximum power in the recumbent pedalling position. Finally, once adjusted, the pilot will need to be trained to peak performance.

The ergometer uses a bicycle-type wheel for inertia and a conventional brake caliper for resistance. Wheel speed is sensed using a magnetic pickoff next to a toothed wheel. Resistance force is measured by a force transducer connected to the brake caliper. Force transducer information is presented in Appendix E. Inputs are to a data card designed for an IBM compatible personal computer. The instrumentation has been acquired but not installed. When complete, the computer will be able to give a real-time display of power versus time and provide a hard copy of the data results.

B. LESSONS LEARNED FROM PAST HUMAN-POWERED AIRCRAFT

In reviewing past projects involving human-powered aircraft, there are many lessons to be learned regarding the operation and logistics of a program such as this. The lessons

regarding design and construction are discussed during the HPH design portion referring to that particular problem.

The project that most resembles this program in terms of scale and degree of sophistication is the Daedalus project. In reviewing that project and that for the Gossamer Albatross, it was surprising that members of both teams felt that the most difficult obstacle was the travel and transportation of the aircraft, crew and support equipment [Ref.4: p.120].

Both the Gossamer Albatross and the Daedalus projects were required to travel to Europe, which consumed the largest portion of their budget. Thus, in comparing the expense and organizational difficulties of a project such as this HPH to these two projects, an HPH will be able to be flown outdoors locally and will not be burdened with the requirement to travel.

Many human-powered aircraft builders were able to get their construction materials from manufacturers in return for some advertising in the form of decals on the aircraft. In a project as significant as this it is anticipated that there would be little problem in obtaining sponsorship from the various companies. In addition, a major helicopter manufacturer allowed Cal Poly to use their filament winding facilities to build their main spar. Although conflict-of-interest rules may prevent this type of sponsorship, it may provide for a source of materials.

When Dr. MacCready built his Gossamer series aircraft, his design was particularly easy to repair. He deliberately designed a degree of crashworthiness into his aircraft during the development stage. This allowed crash damage or design modifications to be easily incorporated and minimized "down" time.

Every successful human-powered aircraft had at least one prototype. There were two Gossamer Condors, a prototype Daedalus aircraft, and three Da Vincis. There is so much to be learned from the construction of the aircraft, that a prototype is crucial to a successful project. A detailed analysis of construction techniques will allow the team to avoid the construction pitfalls of previous aircraft.

The Daedalus team found that an aircraft can be engineered as carefully as possible, but still not perform nearly to the degree anticipated. The Daedalus prototype, called the Light Eagle, was designed to break the Gossamer Albatross distance record of 21 miles. But when it first flew, it could barely stay aloft for three minutes.([Ref.4: p.147] The prototype required a *12-foot* extension on the wingtips and extensive minor adjustments in equipment and technique before it finally was able to be flown over 37 miles. [Ref.4: p.172] It can be seen that construction of a human-powered aircraft represents design in an uncertain flight regime that is so difficult that even this team of experienced human-powered aircraft designers (that had previously won a Kremer Prize!) was still so far off

of their performance goals that their prototype had to be modified with a 12-foot wingtip extension. Designing an HPH requires dealing with infinitely more complicated aerodynamic phenomena than a fixed-wing aircraft and will most certainly require a prototype.

III. AIRCRAFT DESIGN

A. HUMAN-POWERED AIRCRAFT DESIGN THEORY

The fundamental design criterion for human powered aircraft is the limited power output. The power required must not exceed the power available for the HPH to be able to hover. HPH design becomes an exercise in lowering the power required to hover.

Basic momentum theory, which assumes that an infinite number of blades accelerate an inviscid column of air through the rotor disk, shows the power required to hover to be:

$$P_{req} = \frac{W^{3/2}}{\sqrt{2 \rho A_{disk}}} \qquad (3)$$

Where: P_{req} = Power Required

A_{disk} = Area of the rotor disk

W = weight of the helicopter

ρ = density of air

It can be seen that the basic concept is to reduce the weight and increase the effective disk area in order to reduce P_{req}. Even though the HPH will not be an actuator disk, the underlying principles still apply.

Interestingly, even though the power required is not linearly proportional to the total weight, Drela has shown that the power required from the pilot is proportional to the

pilot's weight [Ref.8: p.96]. This is applicable where the weight of the helicopter is roughly one-half of the weight of the pilot. As such, within a reasonable weight range, the determining factor for pilot selection becomes the specific power (power per unit weight) the pilot is able to generate.

Two parameters used to relate helicopter performance are power loading (P.L.) and disk loading (D.L.). Disk loading is comparable to wing loading for fixed wing aircraft. The equations for D.L. and P.L. are:

$$D.L. = \frac{W}{\pi R^2} \qquad P.L. = \frac{W}{P} \tag{4}$$

A typical plot of D.L. versus P.L. for conventional helicopters is presented in Figure 4. For this HPH, the approximate weight will be 250 lb. and a pilot will need to put out approximately one horsepower, making the power loading roughly 250 lb/hp. It can be seen that the D.L. will need to be extremely low to be able to fly! With our pre-supposed rotor radius of 36 feet, the disk loading is 0.061 lbs/sq ft.

It was this concept of lowering the wing loading and getting the power loading very high that made the Gossamer series aircraft such a revolutionary design. By slowing the aircraft down and increasing the planform area, the Gossamer team was able to increase the power loading and make an

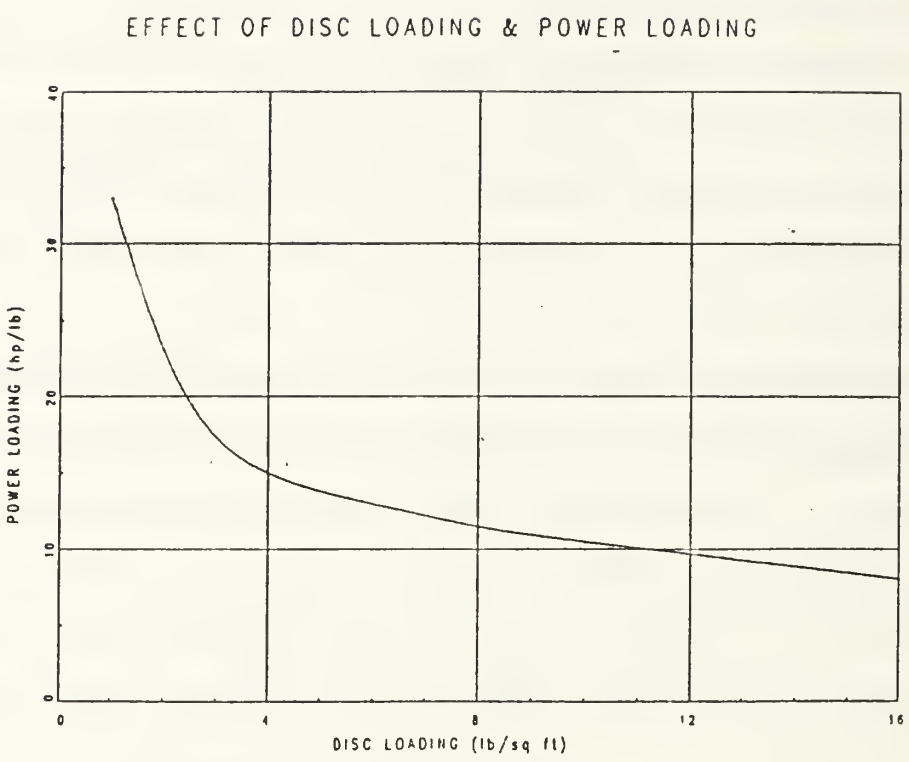

Figure 4. PLOT OF A TYPICAL DISK LOADING VERSUS POWER LOADING FOR A CONVENTIONAL HELICOPTER.

aircraft that required much less effort to fly. So it follows that for this design, the planform area and disk area will be increased as much as are practical, and the power loading will be increased to the point where the power required to hover will be less than one "humanpower!"

B. ROTOR CONFIGURATION

The first consideration in designing a helicopter is the type of rotor configuration to use. The requirement for a tail rotor is an undesirable characteristic, as it represents a substantial amount of energy and weight that is not used for

lift. There are three basic configurations that avoid this requirement: co-axial, tandem and tip-driven.

Grohsmeyer, et al., [Ref.9] evaluated the three designs with respect to stability and control, weight, and efficiency and concluded that a co-axial configuration represented the optimum design.

The co-axial design is superior in all respects except for the higher induced drag on the lower set of blades. It will be shown that that this induced drag is small, but noticeable. The co-axial design then becomes the choice for this design.

C. AIRFOIL SELECTION

1. Preliminary Considerations

The decision as to which airfoil to use is highly influential to the design of this HPH. In determinimg the airfoil to use for the rotor blades, there were two choices: design our own or use one that has already been designed and tested. Both avenues were simultaneously explored, and the results explained in the section below.

2. Airfoil Selection Criteria

In selecting an airfoil for a human-powered aircraft there are four main criteria. All of the criteria except one are driven by the wing construction techniques which are explained in detail in Chapter V.

The criterion not driven by rotor blade construction techniques is the most obvious--high lift-to-drag ratio.

Specifically, the ideal HPH airfoil has a high $C_L^{3/2}/C_D$, referred to as the "power factor." [Ref.8: p.107]

Since the rotor blade is constructed by stretching Mylar over ribs, there cannot be any highly concave surfaces. As the mylar is tensioned it would tend to pull away from the rib. Between ribs the Mylar would not keep its shape but would instead flatten out.

The third criterion is that the airfoil section must be thick enough to contain the blade spar. Since the lightest rotor blade construction uses a main spar for blade rigidity, there must be enough thickness to allow for attaching the ribs to the spar without loosing the stiffness and load carrying capability of the rib.

The fourth criterion is to have an airfoil that is not sensitive to small deviations in shape. The aircraft on the whole is quite flexible compared to conventional aircraft. In addition, the mylar skin of the rotor blades will distort under the dynamic pressure of flight.

There are other criteria in choosing an airfoil section. As in most airfoils, it is not desirable to have a sudden falloff in lift at stall and it is undesirable to have an airfoil that is sensitive to surface imperfections. The shape must be easy to construct within the constraints of a human-powered aircraft. There should not be an excess of volume within the airfoil section as any excess volume adds unecessary weight to the aircraft. An airfoil with as small a

pitching moment as possible is desireable, as the main spar can be designed lighter due to reduced torsion load requirements.

3. Low Reynolds Number Airfoil Design Theory

a. Reynolds Number Defined

Reynolds number (Re) is a dimensionless coefficient that represents the ratio of inertial forces to viscous forces. It is based on a "characteristic" length, which is usually the chord; but can be any length which is characteristic of the flow, such as the boundary layer thickness or momentum thickness. For purposes of this paper, the term "Reynolds number" will imply the Reynolds number based on the chord. At standard sea level conditions, the chord Re is:

$$Re = 6,410 \times V \times C$$

where velocity (V) and chord (C) are in feet per second and feet, respectively.

The Re of a soaring condor and albatross are on the order of 250,000 and 300,000 respectively. [Ref.10: p.204] An A-6E Intruder wing during a low-level flight might have a Re on the order of 50 million. The Re for a helicopter such as an HPH will go from zero at the center to around one million at the blade tips.

b. Drag

Drag on a two-dimensional airfoil has two components: pressure drag and skin friction drag. Pressure drag is caused by a low pressure on an aft facing surface with a resultant component of force acting in the direction of the airflow. Skin friction drag is a result of the viscous forces acting parallel to the surface resisting motion through the medium.

The flow over an airfoil will initially be laminar and then transition to turbulent flow. However, laminar flow is particularly prone to separation. Laminar flow has the lower drag and is therefore the flow of choice for high lift-to-drag airfoils. However, separated-flow drag is orders of magnitude greater than turbulent-flow drag. Laminar flow is extremely sensitive and takes only a very slight surface disturbance to cause separation.

Designing an airfoil becomes a compromise in laminar and turbulent flow. The airfoil should be designed so that it has as much laminar flow as possible to keep drag as low as possible, but should not be designed so the flow is just to the point that any minor disturbance or imperfection will cause separation. The airfoil can be designed with as much laminar flow as practicably possible and then transitioned to turbulent flow before it separates. Controlling transition becomes a major part of airfoil design. Transition can be initiated by controlling the pressure distribution or may be artificially tripped by a mechanical device.

c. Separation Bubble

Low Re airfoil flow is often characterized by the formation of a separation bubble. Under certain conditions the laminar flow will separate, then transition to turbulent flow and reattach--forming a small "bubble." It has been shown that there is a range of Reynolds numbers between 75,000 and 400,000 where the separation bubble dominates the flow and determines the stall behavior [Ref.11: p.108].

If the airfoil geometry is designed carefully, the separation bubble can be used to initiate transition to turbulent flow. If the bubble is kept small the overall drag can be kept lower than the drag resulting from the use of a mechanical transition device.[Ref.12: p.724]

Minimizing separation-induced pressure drag is generally done by minimizing the convex curvature of the upper surface of the airfoil in the transition zone. This results in a very round upper surface.[Ref.10: p.205]

d. Stall Hysteresis

Low Reynolds number airfoils designed for high lift and low drag also characteristically exhibit stall hysteresis. Stall hysteresis is a phenomenon whereby stall inception and stall recovery do not occur at the same angle of attack. This presents a significant problem under stall conditions. If an airfoil stalls, the angle of attack required to re-attach flow to the upper surface may need to be as much as 10 degrees

below that at which the airfoil initially stalled.[Ref.11: p.107]

Stall hysteresis may become relevant with the lower set of rotor blades for a co-axial configuration. The lower rotor blades experience turbulent airflow regimes as a blade passes over top of it, and if this causes separation there may be some stall hysteresis present.

e. Wind Tunnel Testing

There has been relatively little wind tunnel research at Reynolds numbers below about 500,000. This has been primarily a result of relatively little demand for testing within this aerodynamic regime. However, as aerodynamic horizons expand, research in this little-explored regime is increasing. Consequently, the subject is becoming better understood as the need to know the aerodynamic theory increases.

At Reynolds numbers below 300,000, the air flow becomes critically sensitive and difficult to control. Airfoils become extremely prone to separation, and reattachment becomes a function of airfoil geometry and the disturbance environment.[Ref.13: p.763] The disturbance environment in the test section of a low-airspeed wind tunnel is usually determined by freestream turbulence, acoustic phenomena, and mechanical vibrations [Ref.13: p.764].

Boundary layers are prone to transition or separation by disturbances with magnitudes that are on the order of the boundary layer thickness [Ref.14: p.470]--hence the significance of the environmental disturbances within the wind tunnel test section. The wave length of the acoustic noise in the wind tunnel is roughly on the order of the boundary layer thickness, and the acoustic noise, mechanical vibrations and turbulence combine to affect the overall aerodynamic characteristics.

The difficulty in wind tunnel testing comes in separating and/or eliminating the effects of the three disturbances on the performance characteristics of any given airfoil. The ability to precisely perform mearsurements and the procedures used have substantial effects on the results [Ref.13: p.770].

f. Turbulence

As reviewed above, the effects of small-scale environmental disturbances on airfoil performance are significant. It is important to ascertain the effects of larger-scale turbulence (on the order of the magnitude of one chord length). The lower set of rotor blades in a co-axial design operate in the turbulent downwash from the upper rotors. It was desired to be known if the larger-scale turbulence would cause premature separation on the lower set of rotors. For Reynolds numbers on the order of 500,000, "In

order for freestream turbulence to affect turbulent boundary-layer behavior,the length scale must be on the order of the boundary-layer thickness." [Ref.14: p.470] Hence, there is not any detrimental effects of larger-scale on turbulent boundary-layer thickness due to upper rotor turbulence on the lower rotors. In fact, Reference 15 shows that passage of a highly-turbulent pulse over an airfoil at a Reynolds number of 500,000 has a momentary stabilizing effect on the transitional and turbulent boundary layers. The boundary layer is momentarily laminarized before returning to its previous transitional or turbulent state.

g. Summary.

Given the sensitivity of the boundary layer to the disturbance environment, low Reynolds number wind tunnel results become more of a means of comparing airfoils rather than a means of obtaining extremely accurate performance data. As a result, computational analysis is increasingly replacing wind tunnel testing for low Reynolds number airfoils. The airfoils for both the Gossamer aircraft and the Daedalus aircraft were designed using computational methods, and none was ever tested in a wind tunnel before the aircraft flew.

The Daedalus team verified airfoil performance using flow visualization tests on the wing in flight. A mixture of kerosene and black powder dye was coated on the wing. As the kerosene evaporated, the powder was left behind. The laminar

flow left a thick, smooth residue and the turbulent flow left a thin, streaked residue. They were able to see the transition point and compare it to analytical data. Since the transition point matched the computed position, it was assumed that the actual airfoil performance would match the computed performance as well.[Ref.12: p.731]

4. Final Airfoil Selection

Upon reviewing low Reynolds number airfoil design, the author determined that the task of designing airfoils for an HPH would be far too large of a project for a single person to accomplish within the time constraints of this project. The NPS didn't have any on-line programs for airfoil design, and writing one specifically for the purpose of this project, or obtaining a program from NASA would have been prohibitive. Additionally, any new design program woud have to be validated with wind tunnel test data. As a result, it was decided to use already designed and proven airfoils.

The next decision to be made was whether the rotor blade would be aerodynamically tailored or of constant airfoil. An aerodynamically tailored rotor blade would have different airfoils as a function of r/R, with each section having an airfoil optimized for that Reynolds number. In addition to greatly complicating the rotor blade construction, aerodynamic tailoring would have the added requirement to be able to blend one airfoil into another. Additionally, aerodynamic tailoring

would require a tremendous amount of airfoil data at a multitude of Reynolds numbers. Unfortunately, there is just not enough data to be able to compare all of the airfoils at all of the Reynolds numbers available. With the extremely diverse variety of low Reynolds airfoil shapes, blending one airfoil shape into the next would result in unknown airfoil shapes with correspondingly uncertain aerodynamic performance. Consequently, aerodynamic tailoring would only be practical if a "family" of airfoils could be found. With a family of airfoils, the same basic design is modified slightly to optimize performance at different Reynolds numbers. It then becomes reasonable to interpolate between designs to specifically account for the change in Reynolds number along each blade station.

Thus began a thorough search for low Reynolds number airfoils and airfoil data. Other than for human-powered aircraft, low Reynolds number airfoils have been primarily designed for sailplanes and wind turbines. Ref.16 is a compendium of airfoils with performance data at Reynolds numbers of 300,000 and below, and was targeted for remotely-controlled glider enthusiasts. Reference 17 is a compendium of low Reynolds number airfoils and performance data assembled for the Department of Energy for wind turbine use. A few of the potential airfoil candidates are discussed below.

The most obvious source of an airfoil would be from past human-powered aircraft. The Gossamer series aircraft used an

airfoil specially designed for operation at a Reynolds number of 600,000 by Dr. Peter Lissaman. Called the Lissaman 7769 it was also used by the Da Vinci and is shown below:

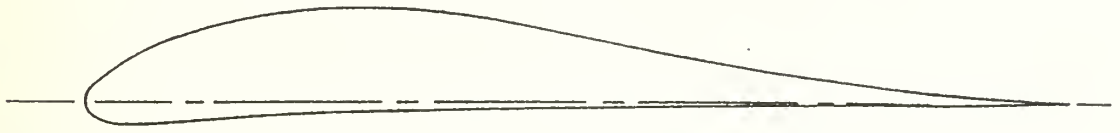

Figure 5. LISSAMAN 7769 AIRFOIL [REF.18]

The Daedalus aircraft used a family of three airfoils designed by Prof. Mark Drela: the DAI 1135, DAI 1336, and DAI 1238 which were optimized for Reynolds numbers of 500,000, 375,000, and 250,000, respectively. The airfoil coordinates are proprietary and not published in this report, but are available for use on the project [Ref.19]. The DAI 1135 has a maximum power factor of 148 at 8 degrees angle of attack with a pitching moment coefficient of -0.12 [Ref.12: p.730].

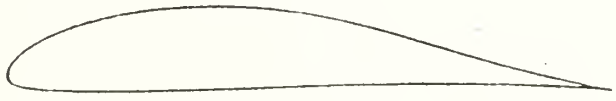

Figure 6. DAI 1135 AIRFOIL [REF.20]

The Gu-25 was designed for high lift and low drag by T. Nonweiler for operation at a Reynolds number of 500,000. It has a maximum power factor of 132. With a zero pitching moment in the "working range," the airfoil has some positive characteristics. But it also exhibits some negative

characteristics--primarily that the airfoil separation drag is very sensitive to surface imperfections. [Ref.21: p.16] The Gu-25 is depicted in Figure 7 below:

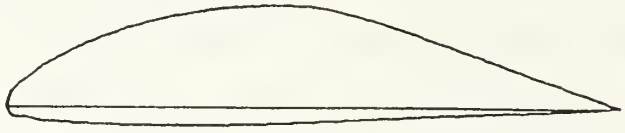

Figure 7. Gu-25-5(11)8 AIRFOIL [REF.17: P.A-348]

A series of airfoils designed in Germany by F.X. Wortmann for high lift exhibit good lift-to-drag characteristics, but the highly reflexed shape leads to difficulty in tensioning and attaching the skin to the concave surfaces. The design also results in a larger pitching moment. One such airfoil, the FX63-137, is depicted in Figure 8.

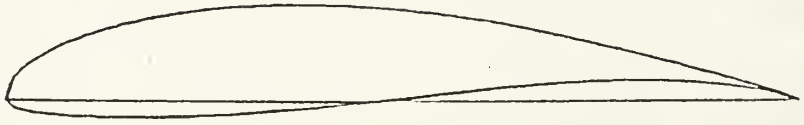

Figure 8. WORTMANN FX63-137 AIRFOIL [REF.17: P.A-102]

Similar to the FX63-137, the FX76-140MP was designed specifically for human-powered applications by Wortmann in 1976. The DAI series have a higher power factor than the FX63-137 and a similar power factor to the FX76-140, but the DAI series has a lower pitching moment than the Wortmann airfoils. [Ref.8: p.106]

Selecting the optimum airfoil was not a clear cut procedure. Power factor data were not available for all airfoils at the same Reynolds number, and some of the merits of the particular airfoils had to be accounted for somewhat subjectively. The airfoils with the best overall characteristics appears to be the DAI series airfoils. They have the highest power factor ($C_L^{3/2}/C_D$), yet have a low pitching moment. Being specifically designed for human-powered aircraft, they are not sensitive to surface imperfections, and have a satisfactory geometric shape for construction purposes. They also afford the opportunity to use the family of three airfoils if necessary. Consequently, the DAI airfoils will be used for the HPH.

D. PLANFORM

1. Preliminary considerations

The overall goal in designing the rotor blade planform was to optimize the design for ease of construction and most efficient lift generation. The ideal rotor blade would incorporate twist and taper; but the easiest rotor blade to construct is one with a constant chord. In order to evaluate the trade-offs between creating the most efficient rotor blade and one that was easy to construct, it was first necessary to determine the variable parameters for rotor blade design. The advantages of each parameter were then balanced against the disadvantages arising from construction requirements.

2. Rotor Diameter

Many human-powered aircraft have had rotor diameters or wing spans determined not by some critical design parameter but by some arbitrary physical constraint such as the width of the hangar it was stored in, or the size of the gym where it was flown! So it follows with this design. The rotor blade length (rotor radius) was initially held fixed at 36 feet, giving the rotor an overall diameter of 72 feet. Arrived at heuristically, this number represented a compromise between length, construction and ease of finding a location for flight. Most importantly, it was approximately the size that Grohsmeyer, et al. concluded with as their design radius [Ref.9].

The 36-foot radius represented a number which was known to be roughly optimum that could be held constant, while all of the other design parameters could be varied. After the design was completed, the performance for a 36-foot rotor radius was very reasonable, so the 36-foot radius was retained as the design radius.

Holding the initial radius constant did not unreasonably constrain the design, as the rotor tips will be designed to be easily modified. It will be easy to add an extension on to the rotor blade if more planform area is needed, or to modify the tip shape. Obviously, it would be easy to shorten the rotor blade should it prove necessary.

3. Twist and Taper

The ideal rotor blade for a hovering helicopter has uniform inflow over the rotor disk, with each section of the rotor blade operating at a constant angle of attack. In addition, profile losses will be minimized if the section is operating at the optimum angle of attack.[Ref.22: p.99]. Hence the section will be designed to operate at the maximum power factor ($C_L^{3/2}/C_D$). In achieving the optimum angle of attack for a hovering helicopter rotor, blade twist and taper (or a combination) may be used to optimize the blade.

Ideal taper for a rotor blade assumes a uniform induced velocity and a constant blade pitch angle. Ideal taper for a four-bladed rotor is shown in Figure 9. The equation for ideal taper is

$$c = \frac{c_{tip}}{r/R} \tag{5}$$

where: c = chord

c_{tip} = tip chord

r = local radius

R = rotor radius

Source:[Ref.22: p.46]

Ideal twist for a conventional hovering helicopter is

$$\Theta = \alpha + \frac{v}{\Omega R} \tag{6}$$

where: θ = blade pitch angle

α = local angle of attack

v = induced velocity

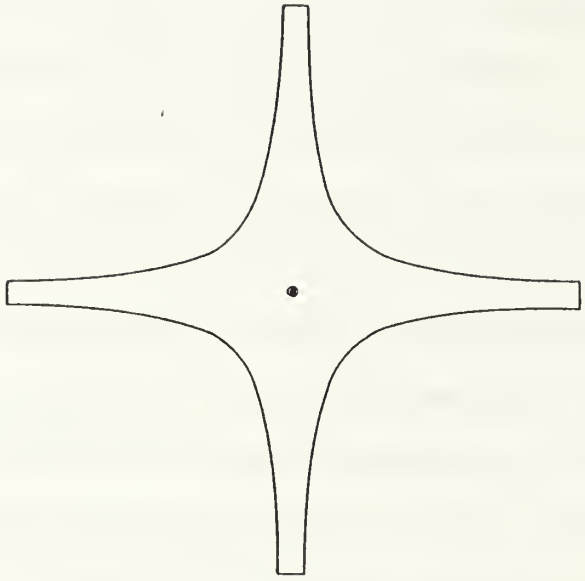

Figure 9. ROTOR WITH IDEAL TAPER [REF.23: P.47]

Ω = rotor speed

r = local rotor radius

Source: [Ref.17: p.46]

Ideal twist also assumes uniform induced velocity. A graph of ideal twist for constant chord blades and for ideally tapered blades is presented in Figure 10.

To get a feel for the magnitude of the effects of taper and twist, Table 1 is presented for a rotor of solidity equal to 0.040 for two torque coefficients (C_Q).

The above results are valid for a rotor solidity of 0.042 to 0.060. It is noteworthy that a linearly twisted and tapered blade is only 2 percent less efficient than an optimum rotor. The optimum rotor is based upon a uniform induced velocity, and an ideal geometry which is impractical and unrealistic for a two-bladed rotor. The apparently small benefit from an

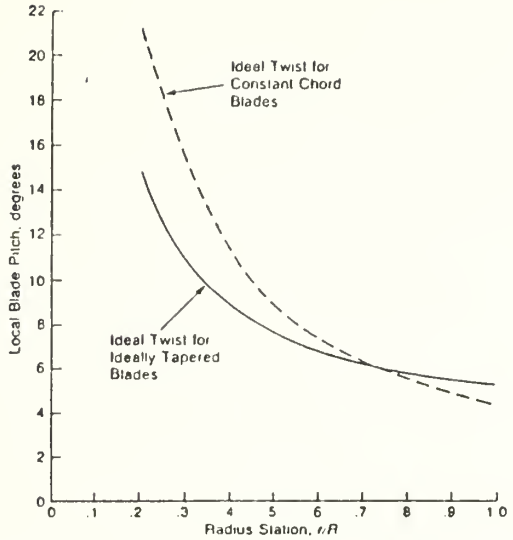

Figure 10. IDEAL TWIST FOR BLADES WITH CONSTANT CHORD AND BLADES WITH IDEAL TAPER [REF.23: P.47]

ideally tapered and twisted rotor is not an adequate tradeoff for a blade that will be significantly more complicated to construct.

Table I. PERCENT INCREASE IN THRUST FROM UNTWISTED AND UNTAPERED BLADE FOR C_0=0.00026 to 0.00044 [Ref.16: p.97]

Blade Twist (degrees)	Blade Taper Ratio	Thrust Increase (percent)
0	3	0
-8	3	5
-12	3	5
Ideal	Optimum	7

In considering the degree to which twist and taper will complicate the rotor blade construction, twist will have the most significant contribution toward complicating the

construction. In making a flat blade it will be easy to lay out the ribs and spar on a flat surface. Having twist will require a different pitch angle for each rib and make laying out, constructing and storing the blade difficult. Hence, the decision was made to investigate designing a blade with taper and no twist.

It can be shown that different blade geometries can be modified to create the same induced velocity profile [Ref.24: p.69]. Thus, taper and twist are interchangeable to create the same blade loading. Twist and planform are interrelated by inflow angle, rotor blade pitch angle and chord, and azimuth. Since this is a point-design for hover, the inflow will be polarly symmetric and there will not be any azimuthal dependency between twist and planform.

It can be shown that little difference exists between a full linearly tapered rotor blade and a blade that is partially linearly tapered over the outboard half [Ref.22: p.97]. Since the outboard sections of the blade contain the majority of lifting surface, this result makes intuitive sense. Therefore, it was decided to use a partially tapered rotor blade.

It was also noted that if the taper were designed effectively, the Reynolds number could be held close over the outboard section. This represented a different approach to designing blades. A quick estimation of induced velocities revealed velocities on the order of 2 to 3 feet per second.

This would compare to induced velocities on the order of 35 feet per second for a large conventional helicopter. A hovering conventional rotor has roughly an 8% to 12% increase in power-required due to an increase in induced drag as a result of nonuniform inflow [Ref.25: p.61]. However, with such low induced velocities it was assumed that the losses from a less-than-optimum inflow distribution would be minimal. Tailoring the rotor blade local chord-Reynolds-number to optimize local airfoil performance might bring sufficient performance returns to offset the loss in efficiency from a non-ideal induced velocity profile.

Designing the rotor blade so that the local Reynolds number remains nearly constant would allow use of one airfoil over the entire rotor blade and simplify construction. As the Daedalus airfoils represented the best overall airfoil available , it was desired to center the Reynolds number around one of those airfoils' design Reynolds number (250,000, 375,000, or 500,000).

After considerable experimentation, the planform shown in Figure 11 was arrived at. The planform represents the geometry that gives the lowest power-required to generate 250 lb of thrust out-of-ground-effect (OGE), and maintains the Reynolds number within 86,000 of 500,000 along the outer half of the blade. The Fortran program used to compute the hover performance is presented in Appendix F and will be referred to as the Performance Program. As the rotor blade design was

designed to performance criteria, further details into the rotor blade design are presented in Chapter IV.

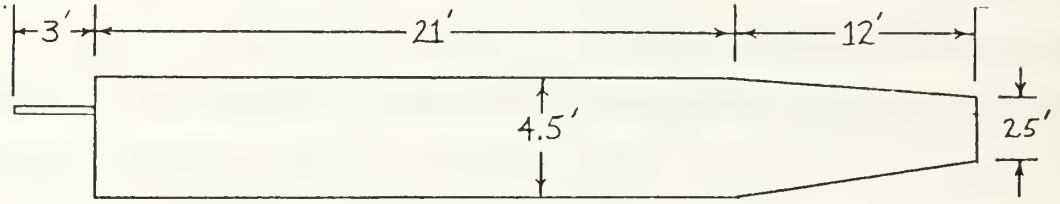

Figure 11. ROTOR BLADE PLANFORM

4. Tip losses

Three-dimensional loss effects at the blade tips are typically modelled using a tip loss factor "B" where the blade is assumed to generate lift out to the radial position B*R. Tip losses are caused by two factors: spanwise flow around the tip of the blade and interaction between the blade tip and the vortex from the preceding blade. Thus, tip loss factors traditionally take two forms: as a function of the tip chord, and as a function of rotor geometry. [Ref. 26: p.69]

Johnson [Ref.25: p.59] offers several commonly used formulas. The first, by Prandtl is:

$$B = 1 - \frac{\sqrt{2\,C_T}}{b} \qquad (7)$$

where: C_T = rotor thrust coefficient

b = is the number of rotor blades

Two similar formulas by Wheatley and Sissingh respectively are:

$$B = 1 - \frac{C_{tip}}{2R} \tag{8}$$

and,

$$B = 1 - \frac{2C_{tip}}{3R} \tag{9}$$

Tip loss is proportional to the strength of the trailing tip vortex. The tip vortex results from roll-up of the trailing vortex sheet into a tip vortex. The trailing vortices are proportional to the rate of change of bound circulation ($d\Gamma/dr$) [Ref.25: p.76]. Since the bound circulation for a blade of a conventional helicopter is much higher than this HPH rotor blade (which is of comparable size), and $d\Gamma/dr$ is much smaller than for a conventional helicopter, it is expected that the tip losses will be smaller than might be calculated by any of the above means. In order to be conservative, the blade tip loss factor by Prandtl was used. It still has been proven to be an accurate tip loss factor, yet it gave the least amount of tip loss.

IV. PERFORMANCE

A. HOVER PERFORMANCE

1. Hover power calculations

Several fundamental assumptions were made in the initial performance calculations. During the initial phases of design, sizing and performance estimates, hover power calculations were made for the 3-meter height hover condition. This was considered to be out of ground effect. This assumption was made due to the low disk loading of the HPH rotor. In normal practice, out of ground effect is taken at a one rotor-diameter height. Typically, graphs generally indicate that ground effect would provide significant benefit on hover performance. In this case, the extremely low induced velocities were assumed to negate ground benefit. This also represented a worst case scenario and yielded conservative estimates.

The rotor speed is slow enough that it was assumed that the inflow from the preceeding blade will have decayed to a negligible magnitude by the time the trailing blade arrives. Thus, the pitch angle was deemed equal to the angle of attack. The influence of the inflow from the upper blade will cause a momentary reduction in the angle of attack as it passes over the lower blade. However, for the sake of simplicity in the

initial design, inflow on the lower blades was neglected. The validity of these assumptions will be evaluated later.

Initial hover power estimates were from the Performance Program which makes use of blade element theory. The program assumes a linear taper over the outer one-third of the blade and constant chord over the rest of the blade with a 3-foot offset. The program also calculates two tip loss factors (B) and uses the larger one (least amount of tip losses). User inputs are rotor radius, root chord, tip chord and rotor RPM. Program output is blade station, chord, and Reynolds number into a data file, "Reynold.Dat." Thrust, in-plane drag and induced velocity versus blade station are input into files "Thrust.dat", "Drag.dat" and "Indvel.dat", respectively, for plotting.

The tip loss factor generated by the program for the final configuration was 0.965, yielding an effective blade length of 34.74 feet. The rotor blade was divided into 30 sections of 1.2 feet each so that the outboard section corresponded to the length of rotor blade which was truncated.

The final blade geometry selected was:

- Rotor radius - 36 ft
- Root chord - 4.5 ft
- Tip chord - 2.5 ft
- Rotor speed - 8 rpm

The rotor blade design was based primarily on two criteria: keeping the chord Reynolds number fairly constant over the outer half of the blade, and the minimum diameter to keep the power at or below 1.5 hp. The goal during the design process was to keep the chord Reynolds number within +/- 100,000 over the outer half of the rotor blade, enabling the use of one airfoil. The final design keeps the Reynolds number within 86,000 of 500,000 (which is the design Reynolds number of the DAE 11 airfoil). A table of data showing the Reynolds number versus the blade station is presented in Table B-1, Appendix B.

The rotor blade configuration above results in the following performance:

- Total thrust - 250 lb
- Power required - 1.53 hp
- Tip speed - 30.5 fps
- Tip loss factor - 0.965

The tip loss factor closely correlates with that used for conventional helicopters which is often taken to be a constant 0.97. The taper ratio was used primarily to keep the Reynolds number as constant as possible. Of all of the rotor blade parameters, the rotor radius has the single greatest effect on aircraft performance. Several rotor radii are presented in Table II to get a feel for the relationship between radius and horsepower required to generate 250 lb of thrust for a blade

with the same relative geometry (1.8:1 linear taper over the outboard 33%). It can be seen that the relationship between rotor radius and power required is linear at 0.0167 hp/ft.

Table II. POWER REQUIRED TO GENERATE 250 LBS OF THRUST FOR VARIOUS ROTOR RADII.

ROTOR RADIUS (ft)	POWER (hp)
28	1.74
32	1.63
36	1.53
42	1.43

2. Vortex lattice method

The vortex lattice method (VLM) described in [Ref.28: p.271] was used to calculate the lift over the rotor blade. Only one chordwise horseshoe-vortex was used. The Fortran program used is presented in Appendix F. The vortex distribution is presented in Figure A-1, Appendix A. The same basic airflow assumptions as for the blade element program were made in the vortex lattice program. The final geometry from the blade element method was used and a total lift of 71 lb per blade (284 lb total) was calculated. This represented an 11% increase in lift over the blade element method. The VLM lift distribution is plotted along with the blade element

method in Figure A-2, Appendix A. A table of circulation versus blade stations is presented in Table B-2, Appendix B.

The VLM is presented as a separate method to verify the results of the blade element method. The VLM method is assumed to be less accurate and is not used for primary performance calculations. However, the lift distribution is much more accurate and will be useful for structural considerations.

3. Approximation accuracy

a. Pitch angle equal to the angle of attack

This section will make some simple flow models and estimate the degree to which some of the basic assumptions were valid. The assumption was made that the pitch angle was equal to the angle of attack. This implied that the induced velocity of the leading rotor blade will decay to approximately zero before the next blade arrives at that azimuthal position. Or, from another perspective, this assumption says that each blade is moving into "clean air," that is, air undisturbed from the previous blade. To estimate the validity of the assumption, assume that the trailing streamlines are that of flow over a rotating cylinder where the diameter is equal to the chord. The equation for the radial velocity around a cylinder is given by:

$$V_\theta = -(1 + \frac{R^2}{r^2}) V_\infty \sin\theta - \frac{\Gamma}{2\pi r} \qquad (10)$$

If the tip path plane is considered as $\theta=0$ then V_θ is the induced velocity, and the induced velocity becomes:

$$v_i = -\frac{\Gamma}{2\pi r} \qquad (11)$$

The negative sign implies that with a positive circulation the tangential velocity is clockwise for flow from the left, and that the induced velocity is in the downward direction.

A graph of induced velocity versus rotor blade station is presented in Figure A-3, Appendix A, and is typical of a conventional rotor blade profile. The maximum induced velocity of 2.1 fps occurs at 25.27 ft which corresponds precisely to 0.7R. Since a lower blade has an upper blade pass over it four times every revolution, there will be one-quarter of an arc of distance behind the lower blade until the next upper blade passes over it. At 0.7R, the one-quarter arc distance will be 39.6 ft.

At 0.7R, the calculated induced velocity is 2.1 fps and using equation 3 above with a radius of one-half of the chord, the circulation is 29.7sq ft/s. This compares to a value of 33.6 sq ft/s, which was calculated for the VLM. As the VLM calculated 11% higher lift, a higher circulation from the VLM would be anticipated (111% of 29.7 is 32.9). Using the value of circulation calculated from the induced velocity

(Γ=29.7 sqft/sec.), at 79.2 ft behind the blade (two times the quarter-arc distance of 39.6 ft) the induced velocity (v_i) becomes 0.060 ft/sec when the next blade passes under it. The inflow angle becomes:

$$\phi = \frac{V_i}{\Omega r} = 0.16 degrees \qquad (12)$$

The rotor blade pitch angle can be trimmed to operate at an average angle of attack closest to the optimum power factor so the induced velocity will not adversely affect the lift generated. Rather, it will mean that the blade will be tilted aft slightly (0.16), increasing the component of the lift vector in the in-plane (drag) direction. This calculation is based on the largest induced velocity and is small enough to be considered insignificant with respect to the anticipated torsional flexibility of the rotor blades.

b. Inflow on the lower set of rotor blades

To obtain an estimate of the effect of the previously neglected inflow of the upper rotor on the lower rotor blades, several simple approximations will be made based on the induced velocity of the upper set of rotors. The results will then be applied to the performance program and compared to the originally calculated performance.

Induced air flow passes through the tip path plane at an induced velocity of v_i. The flow necks down and the inflow increases to $2v_i$ at one rotor-diameter below the tip path

plane. The lower set of rotors will be as close as possible below the upper set of rotors, so the increase in induced velocity due to the necking down will be assumed to be negligible.

At 0.7R, where the highest induced velocity is located, a rotor blade passing below this blade will be momentarily subject to an inflow angle corresponding to:

$$\phi = \tan^{-1} \frac{V_i}{\Omega r} = 5.7 degrees \qquad (13)$$

which will effectively reduce the angle of attack by that amount.

To get a feel for the added power required due to the inflow from the upper rotors, a simple flow model is generated, the increase in pitch angle to overcome the inflow is calculated, and the value of that increased pitch angle is put into the performance program to provide an estimate of the additional power required.

Assume that as the leading edge of the rotor blade passes over the lower blade the effective induced velocity increases exponentially according to:

$$V_i(x) = V_{i_{calc}}(1 - e^{-x}) \qquad (14)$$

until the full induced velocity is reached at the trailing edge of the airfoil. This is an assumption based on the induced velocity buildup for a suddenly applied angle of attack on an airfoil [Ref.29: p.4]. After the trailing edge

passes the lower rotor blade, the induced velocity decreases according to that of a cylinder of diameter equal to the chord. The complete formula to calculate the induced velocity becomes:

$$v_i(x) = v_{i_{calc}}(1 - e^{-x}) \quad 0 \le x \le c \tag{15}$$

$$v_i(x) = -\frac{\Gamma}{2\pi r} \quad c \le x \le 39.6 \tag{16}$$

Integrating over the entire quarter of arc and dividing by the length of the arc to find the average induced velocity yields:

$$v_{i_{avg}} = 0.416 fps \tag{17}$$

Using equation 13, the average inflow angle becomes:

$$\phi_{avg} = 1.61 \ degrees \tag{18}$$

Again, this implies that the lower set of blades will have to have the pitch angle increased 1.61 degrees to operate at the same average angle of attack. Adding the increased inflow angle to the pitch angle will tilt the lift vector further aft resulting in a higher in-plane drag. Adding the increased inflow angle to *phi* in line 84 of the performance calculation program will increase the pitch angle on all four blades. With *phi* equal to 1.68 radians, the program calculates an increase in power required from 1.53 hp to 1.82 hp. Since only half of the blades will show an increase, the average of the two results in a power required to hover of 1.68 hp. This

represents an increase in power required of 0.15 hp, or a 10% increase.

A power increase of 10% represents a noteworthy increase. However, it will be seen that it is not too significant when compared to the variables associated with ground effect.

B. GROUND EFFECT

1. Theory

Ground effect is defined as a reduction in induced power due to proximity of the ground. It is characterized by a reduction in induced velocity required to produce a given thrust. A plot showing induced velocity ratio as a function of normalized rotor height is presented in Figure 12.Since the induced velocity is reduced in ground effect for the same thrust generated, the blade can operate with the same angle of attack at lower pitch angles. The reduction of pitch angle results in less rearward tilt of the lift vector, and consequently a reduction in the induced power from that required out of ground effect. Height above the ground is typically referred to as Z/D, where Z is the rotor height and D is the rotor diameter.

The difference in power required due to ground effect becomes:

Where: v_1=induced velocity

Source: [Ref.25: p.67]

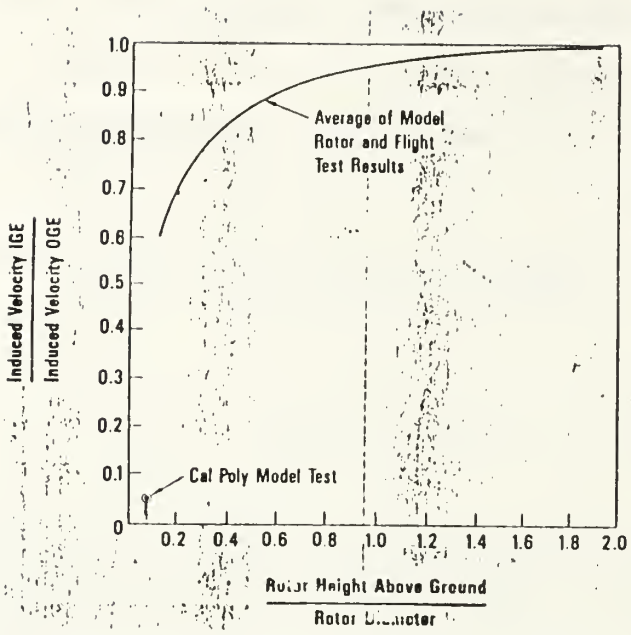

Figure 12. INDUCED VELOCITY RATIOS [REF.31: P.6]

$$\Delta h.p. = \frac{TV_{1_{OGE}}}{550}\left(1 - \frac{V_{1_{IGE}}}{V_{1_{OGE}}}\right) \qquad (19)$$

Betz (1937) obtained a ratio for power in ground effect for $Z/R < 1$ [Ref.25: p.123] where:

$$\frac{P_{IGE}}{P_{OGE}} = 2\frac{Z}{R} \qquad (20)$$

Ground effect is also depicted using the ratio of thrust-generated-in-ground-effect to the thrust-generated-out-of-ground-effect (for constant power) versus normalized rotor height (Z/D). Figure 13 presents such a graph.

Recent investigations by Cal Poly students have shed some light on this unexplored regime of flight, and resulted in the "Cal Poly Model Test Point" on the classic graph. Tests show a continued reduction in induced velocity well below where

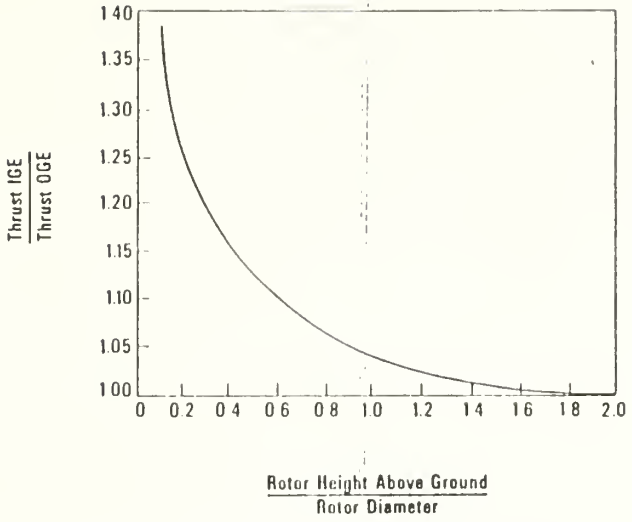

Figure 13. THRUST FOR SAME POWER [REF.31: P.5]

most graphs and data go. This is shown on Figure 12, above. This implies that at very small Z/D, rotor drag becomes primarily profile drag.

Interestingly, tests at Cal Poly by Baker and Scarcello show increased ground effect over rough surfaces. Hence, when the Cal Poly team was attempting to achieve the world's first human-powered helicopter hover, they put relatively large cardboard fences on the floor in an attempt to increase the "surface roughness" of the gym floor and take advantage of this surface roughness effect. [Ref.28: p.6]

With the exception of recent studies at Cal Poly, there has been little, if any, research on helicopter rotors deep in ground effect. The standard configuration of most helicopters places the rotor already at Z/D of roughly 0.2 when sitting on the ground. This has probably obviated the need for studies of ground effect below that Z/D.

2. Ground Effect Calculations

a. 3-meter height

The initial hover power calculated assumed that at the 3-meter height the rotors were out of ground effect. For a preliminary rotor height consideration, assume that the rotor blades will be co-located 5 ft above the bottom of the HPH. The rotor height at the competition 3-meter height requirement then becomes approximately 15 ft and Z/D=0.21. Entering Figure 13 shows a thrust ratio of 1.26. This indicates a 26% thrust improvement for a given power over the true OGE calculation. If this condition held true, the power required to hover at the 3 meter height would be 1.33 hp.

Assuming that the two sets of rotor blades are 4 feet apart, then:

$$\frac{Z}{D}_{lower} = \frac{13}{72} = 0.18 \qquad \frac{Z}{D}_{upper} = \frac{17}{72} = 0.24 \qquad (21)$$

and

$$T.R._{lower} = 1.27 \qquad T.R._{upper} = 1.24 \qquad (22)$$

showing that there might be a 3% differential thrust for a blade separation of 4 ft with airframe height of 3 meters. Within the accuracy of the theory, 3% is not deemed significant and will be disregarded for IGE performance calculation purposes, but will be important for control purposes.

Entering Figure 12 with Z/D of 0.21 gives a value of the induced velocity ratio of 0.7. Equation 19 assumes that the induced velocity is constant over the blade, so the average induced velocity generated from the Performance Program will be used to calculate ground effect. Using average induced velocity of 1.67 fps, the Δhp is 0.23 hp, and the power required to hover IGE becomes 1.30 hp.

b. Deep In Ground Effect

Using Betz's formula with the true OGE hover power calculation and the added induced power on the lower set of blades:

$$P_{IGE} = (P_{OGE})\, 2\, \frac{Z}{R} = (1.68)\,(2)\,(\frac{6}{72}) = 0.56hp \qquad (23)$$

Using:

$$\frac{Z}{D} = \frac{6}{72} = .0833 \qquad (24)$$

the hover situation approximates the "Cal Poly Point" on Figure 12. The ratio of induced velocities is 0.05. Using the average induced velocity (provided by the Performance Program) of 1.67 fps, the Δhp is 0.72 hp; making the power-required to hover IGE 0.80 hp.

c. Summary of Ground Effect Calculations

The basic assumptions made in calculating hover power were: the inflow from a rotor blade will have decayed to zero at the trailing blade; inflow effects on the lower set of

Table III. SUMMARY OF HOVER POWER CALCULATIONS FOR HPH.

ASSUMPTIONS	POWER (hp)
--3-meter height--	
Basic assumptions, true OGE.	1.53
Basic assumptions, inflow effects on the lower set of rotors, OGE.	1.68
Basic assumptions, inflow effects on lower rotors, IGE using Figure 12.	1.30
Basic assumptions, inflow effects on lower rotors, IGE using Figure 13.	1.33
--Just clear of the ground--	
Basic assumptions, inflow effects on lower rotors, Betz's formula.	0.56
Basic assumptions, inflow effects on lower rotors, "Cal Poly Point."	0.80

rotor blades were neglected; and the 3-meter hover height was out of ground effect. The Performance Program calculations were based on blade element theory and used the tip loss formula by Wheatley. A summary of hover performance calculations is presented in Table III.

C. STABILITY AND CONTROL

The importance in having an aircraft that is controllable is critical to this competition. It will not be possible to build an aircraft with the inherent stability to meet the requirements of the Igor Sikorsky Award. Just as the introduction of the swashplate enabled Igor Sikorsky to obtain

satisfactory control and achieve the first truly successful powered flight of the VS-300 helicopter in 1939, the "control problem" must be accounted for in the HPH design. As was seen in the introduction, it was controllability that allowed the Gossamer Condor to become the "first" human-powered aircraft. In their case, the unstable nature of their design was not a problem, as the controllability characteristics were such that the pilot could easily maintain steady flight. During the Da Vinci's 7-second world-record flight, it appears that the pilot could have easily flown longer, but the aircraft was becoming increasingly unstable and in imminent danger of crashing. A controllable aircraft is paramount to a successful human-powered hover, and winning the Igor Sikorsky Award.

1. Controllability

> "Controllability may be defined as the capability of the helicopter to perform, at the pilot's desire, any maneuvering required in a particular mission. The characteristics of the airplane should be such that these maneuvers can be made precisely and simply with a minimum of pilot effort. [Ref.32: p.2-2]"

In this case the "mission" is to maintain a hover within the prescribed area and maintain a constant heading for one minute. It can be seen from this definition of controllability, that if the aircraft is unstable but easily controllable, the flying qualities could still be satisfactory for the mission. Today's powered helicopter (without automatic stabilization) is in this control category.

2. Static Stability

An aircraft is statically stable if it tends to return toward its original trimmed condition when disturbed from an equilibrium condition [Ref.32: p.3-3]. An aircraft is dynamically stable if it returns to an equilibrium condition on its own if disturbed from trim [Ref.32: p.3-4]. Both definitions are open-loop conditions, whereby the controls are left in the trimmed position and the pilot does not make any inputs to correct the aircraft attitude.

An aircraft can be statically stable but dynamically unstable. An example would be an oscillatory motion of increasing amplitude called "oscillatory divergent". It tends toward returning to trim but overshoots by an increasing amplitude each cycle. To be dynamically stable, the aircraft must be statically stable.

Positive damping is that characteristic of a system which opposes transient motions and results in decreasing cyclic amplitudes (for oscillatory motion) or decreases a rate of motion [Ref.32: p.3-5]. Negative damping is unstable. Classically, a damping force or moment is proportional to velocity, and in some non-linear cases to $(\text{velocity})^2$. Hence, roll damping is the moment which opposes a roll rate and causes the aircraft to stop rolling once the controls are returned to neutral.

Light, large aircraft such as human-powered aircraft have low inertia and very high damping compared to conventional

aircraft. The pitch damping of the Gossamer aircraft was high enough that the maximum rates that could be developed (if allowed to diverge) were so small that they were easily compensated for by the pilot. If an aircraft is unstable, it is important that adequate control margin is available to be able to control the aircraft.

Associated with unsteady aerodynamics, there is an inertia force referred to as "apparent mass." When accelerating a wing perpendicular to its direction of motion, it is necessary to accelerate not only the wing itself but the air surrounding the wing as well. For a high aspect ratio wing, the apparent mass is equal to the mass of a cylinder of air with a diameter equal to the local chord. For the rotor blade design proposed:

$$AM = \pi \left(\frac{C_{rt}}{2}\right)^2 (24)\, \rho_{air} + \frac{1}{2}\pi \left[\left(\frac{C_{rt}}{2}\right)^2 + \left(\frac{C_{tip}}{2}\right)^2\right] (12)\, \rho_{air} = 38.8\, lb$$

Each rotor blade weighs approximately 20 lb. Thus, the apparent mass nearly doubles the inertia of the rotor blade. Despite the increased inertia, Drela [Ref.8: p.104] showed that roll damping still dominates the roll response in human powered aircraft.

A generic helicopter in a hover will be statically stable with regard to translational velocity [Ref.22: p.283]. That is, if the trimmed hovering aircraft is displaced in roll it will not generate a restoring moment until a translational velocity is developed which causes blowback which generates a restoring moment. If allowed to continue unchecked in a

conventional helicopter, the motion results in a dynamically unstable oscillatory divergence [Ref.23: p.603]. In a HPH, the pitch and roll damping are so high that large rates cannot build up. It is anticipated from dimensional considerations that this HPH will be statically stable as well. If allowed to start, an oscillation in pitch or roll would be of limited amplitude due to the limited pitch/roll rates. However, the aircraft would tend to "slide" sideways into the ground. As such, it will be imperative that a control system be implemented to keep lateral and longitudinal translational velocities to zero.

3. Lateral and Longitudinal Control

It is proposed that a side force generator rather than a roll moment generator be used to control the HPH. The basis for this proposal is the trouble exhibited by past human-powered aircraft in roll control. There will be very little difference between roll and pitch for this aircraft, so "roll" will be used to imply either pitch or roll. The wings of past human-powered aircraft have been so flexible that conventional aileron control has been ineffective. For turns, the Gossamer series used a canard as a yaw force generator to generate differential wing lift and consequently a roll moment. The Daedalus team was unable to make an effective aileron system so they used the rudder and the dihedral effect to make shallow turns.

Rotor blade winglets on the upper set of blades are proposed as the means of generating a side force. By cyclically varying the angle of incidence of the winglets a side force can be generated and used to control position over the ground. If designed correctly, winglets may also have the added benefit of reducing tip losses.

4. Directional Control

Heading control will also be necessary to win the competition. Torque differentials between two rotor blades caused by inflows, non-linear ground effects, and winglet inputs will cause the pilot to rotate with reference to the ground. Conventional heading control for counter-rotating rotors is by differential collective inputs to the two rotors. Heading control for this HPH is proposed by changing the torque on the upper rotor only. This can be performed by changing the total lift on the upper rotor. The rotors can be finely tuned so as to be in torque balance for one flight condition, thus requiring only small inputs to maintain heading as hover conditions vary. Lift change on the upper rotor can be accomplished by either a small flap-type control or by blade pitch change.

The co-axial design has an inherent stability advantage over a two-bladed helicopter in that it has polar moment of inertia symmetry between X and Y axes. For the Da Vinci, $I_{xx} > I_{yy}$. The extremely small moment of inertia about the

feathering axis resulted in the helicopter pitching about the main spar (feathering axis) and falling over.

5. Collective Control

The most simple means of controlling thrust (for height control) is by varying rotor speed. It has the advantage of eliminating mechanisms required to feather the blades and thereby reducing total airframe weight. Some radio-controlled helicopter models have been very successful in using this technique to eliminate the conventional collective control.

6. Energy Storage

An investigation was made into using the inertia of the rotor blades to store energy. If a system were derived whereby the blades could be held at the zero lift angle of attack, the blades could be accelerated to above the design speed and the energy in the rotor inertia could be used to help lift the aircraft to the 3-meter height immediately after takeoff. Considering only the inertia of the rotor blades, the total inertia is the sum of the two sets of blades where the blades are assumed to have uniform mass distribution. The moment of inertia of a long uniform rod rotating about the middle is:

$$I_{yy} = \frac{1}{12} m l^2 \qquad (26)$$

where for this case: m = 40 lb

l = 72 ft

and

$$I_{yy} = 17{,}820 \ lb\text{-}ft^2 \tag{27}$$

The energy required to lift 250 lb to 3 meters is:

$$P.E. = mgh = 80{,}500 \ \frac{ft^2\text{-}lb}{s^2} \tag{28}$$

The kinetic energy in the rotor system is:

$$K.E. = (2)\frac{1}{2} I\omega^2 = 12{,}514 \ \frac{ft^2\text{-}lb}{s^2} \tag{29}$$

Assuming the rotor blades will need to be at the design operating rpm at the top of the climb, the total energy needed to be stored in rotor inertia at flat pitch is the sum of the potential energy required to climb to 3 meters and the kinetic energy of the rotors at the design condition. The total energy required at flat pitch is:

$$E_{total} = 93{,}014 \ \frac{ft^2\text{-}lb}{s^2} \tag{30}$$

Solving for the rotor speed required at flat pitch:

$$\omega = 2.18 \ \frac{rad}{sec} = 20.8 \ RPM \tag{31}$$

This would present a problem in that the pilot would be required to pedal at 234 rpm (without any variable gear ratio), an unrealistic speed.

If the maximum flat pitch rotor rpm were limited by profile drag, and a limit of 1 hp were set, then a maximum rotor speed could be calculated using the Performance Program. Unfortunately, airfoil data are only available to 0 degrees

angle of attack (as opposed to the zero-lift angle of attack). The program gives 9.3 rpm at 1 hp; but 125 lb of thrust is still being generated. Regardless, it will not be possible to achieve a rotor speed of 20.8 rpm!

For argument sake, it will be assumed that a rotor speed of 12 rpm would be able to be generated by placing the rotors at the zero-lift angle of attack. Then, by increasing the blades' inertia using tip weights it would still be possible to achieve the added energy at minimum pitch. Solving for the weight necessary to do this results in 34 lb. tip weights--obviously an unrealistic proposition as the power required to hover deep in ground effect with the extra 132 lbs is well above human power capabilities.

In conclusion, the high rotor blade profile drag prevents a high minimum-pitch rotor speed and precludes any effective use of the rotors as a means for storing energy. There would be no advantage in adding tip weights, and no reason to add the capability to feather the rotor blades for energy storage purposes.

V. FINAL CONFIGURATION

A. CONSTRUCTION

The design of an HPH is a relatively simple operation compared with monumental task of building the HPH. Construction will command an extraordinary amount of manhours, require innovative thinking and use of materials not normally used in the aerospace industry. It may be possible to make use of some of the local high school or college students to help construct the aircraft in exchange for science credits. In the attempt to construct a light, strong aircraft, past teams have required a large amount of trial and error in construction techniques. Mr. P. Zwann, builder of two (unhoverable but not unsuccessful) human-powered helicopters, said that probably the best advice he could give was to "...sketch with your materials. [Ref.33]"

As in all arenas of scientific endeavors, progress is made by building upon others' past discoveries, research and development. Through exhaustive research it is hoped that the lessons of past mistakes of human-powered aircraft designs and construction will be learned and not repeated here. This section will discuss some of the construction methods and materials necessary for construction of this HPH.

B. MAIN SPAR DESIGN

1. Composite Technology Background

Composites have been used in aircraft in the form of plywood since the early days of aviation. Advanced composites have allowed significant structural advantages for human-powered aircraft. Good composite design can allow a significant weight savings over other materials and result in a stronger and stiffer structure. Furthermore, it is possible to do much of the composite construction at the NPS without having to resort to a commercial composite outfit. For example, a gentleman named Juan Cruz (who is now a composite specialist for NASA) hand built the spars of the Daedalus aircraft using pre-impregnated unidirectional graphite-epoxy tape [Ref.2: p.97].

Part of the purpose of this HPH project is to promote various aspects of aeronautical engineering. The use of fiber re-inforced composites has been called the biggest technical revolution in aviation since the jet engine [Ref.34: p. 85,90 and 91]. Composite design and construction is becoming an integral part of naval aviation, and as such should be understood by all aeronautical engineers. With some easily constructed facilities at the NPS, it would be quite possible to build the rotor blade spars required for this HPH.

To determine the feasibility and reliability of a hand layed composite section, information from a NASA report

regarding cylinders tested in strictly compression is presented. The report tested HS-4 graphite and 3502 epoxy cylinders with different lay-ups. Despite only reporting on compression test samples, there should be no reason that the quote would not apply to cylinders in combined loading. "A comparison between filament wound and hand laid-up tape control cylinders indicates there is little or no difference in the response of cylinders constructed using the two manufacturing techniques." [Ref.35]

A composite consists of two or more dissimilar elements combined on a macroscopic scale to create a material exhibiting properties that neither has of its own. The material comprising the composite are termed the "constituents." For purposes of this paper, the term "composite" will imply a fibrous composite. A fibrous composite consists of fibers in a matrix. The fibers are long and continuous, and can be woven or unidirectional. The matrix is the substance that binds the fibers together and serves many purposes; among them to add structural support, transfer stresses, and to protect the fibers. The composites can be layered with the fibers in different directions, and the composite becomes a "laminated fibrous composite." [Ref.36: p.2-5]

2. Composite Tube Construction

Cylindrical composite tubes are created by wrapping the composite around a form called a "mandrel." Two main methods are used. Where the facilities are available, tubes are generally constructed using a technique called "filament winding." Here, an individual fiber is coated with a matrix and wound in pre-determined directions, and layers, around a mandrel. The other method is to use pre-impregnated tape called "pre-preg" which comes in rolls or sheets and is wrapped around the mandrel in the same manner as filament winding. Filament winding is generally used for highly automated production, and pre-pregs are frequently used for small batches or one-of-a-kind construction. The composite shrinks upon curing, and extraction of the mandrel becomes difficult. A common method is to etch a groove through the tubular metal mandrel with acid, allowing the mandrel to compress and be easily extracted.

3. Composite Material Selection

In determining the constituents, several factors need to be considered: strength-to-weight ratio, stiffness, and cost/availability.

Graphite represents a strong, stiff and relatively cheap fiber and is probably the most suitable for construction of the main spar. Graphite-epoxy pre-preg unidirectional tape represents the most suitable composite material. In

determining the directions of the individual lamina, called the lay-up, the blade loading will be needed. The thrust and drag have been previously been presented, but the pitching moment has not. The moments are generated by the Performance Program (Appendix F) and the data output to a file "moment.dat." Note that the pitching moments are negative, indicating a leading edge down pitching moment.

Much of composite strength and reliability is dependent upon the manufacturing process. It will be necessary to build and test specimens in order to refine the design and fabrication process. The spar is essentially a torque tube with longitudinal structural re-inforcement on the top and bottom. The Daedalus used smaller tubes bonded to the top and bottom as tension and compression members. The Da Vinci used a lamina running axially (lay-up angle of 0 degrees) on the top and bottom to serve the same purpose.

There exists a flat, unidirectional laminate used by makers of skiis and composite bows that may be suitable as the spar tube cap. Sold by Gordon Plastics in Vista Ca., it is called "Spar Tuf" and comes pre-cured and ready to be bonded. It has been tested in both tension and compression to 150,000 psi.[Ref.37: p.9-4]

4. Bending to Torsion Coupling

The spar can also be designed to incorporate bending to torsion coupling. This would have two advantages. The first

would be to counter the pitching moment. The second would be to serve as an effective collective control to increase the pitch angle as more lift is generated and the blades flex up. Thus, at low speed, the blades would be at a reduced angle of attack and require less torque to accelerate the rotor system. As the lift increases, the blades flex up, and the pitch angle will increase until equilibrium is reached whereby the airfoil is operating at the design angle of attack. Either a section at the root can be designed with bending to torsion coupling so the entire spar twists a constant amount, or the the coupling can be incorporated into the entire blade, inducing blade twist. The former is equivalent to the well known delta-3 hinge built into rotor blades for pitch-flap coupling.

Refinement of the spar design is beyond the scope of this report and is left for follow-on work. The intent is to show that design and construction of a graphite-epoxy spar is well within the capabilities of the NPS.

C. ROTOR BLADES

This paper has used the helicopter terminology of rotor blades, when in fact they are more correctly termed "rotary wings" as strutural rigidity is achieved through a cantilevered spar rather than from centrifugal forces. The Cheyenne and ABC helicopters also had cantilevered rotor blades like this. It gave rise to the term "rigid rotor." That term was considered incorrect, which led to the term

"hingeless rotor." Hence, construction methods will be similar to wings of past human-powered aircraft. Construction of the spars was addressed previously and will not be discussed in this section.

The rotor blades will be constructed using a tubular composite main spar with lightweight ribs, and covered in a thin polyester film. Ribs can be fabricated from low density (2 lb/ft^3) foam and structural support added as necessary. One source for sheet foam is Ref.38. The foam ribs can be backed with paper, or supported with flat composite strips glued to the sides. The leading edge of the rotor blade should have a rigid sheet of material wrapped around it to add rigidity to the skin along the portions of the airfoil with a high (or low) co-efficient of pressure to prevent excessive airfoil deformation.

The polyester-film skin can be made of 0.5 mil Mylar (manufactured by DuPont) which has been used successfully in past human-powered aircraft. Information on Mylar is provided in Appendix G.

The rotor blades need to be designed for easy transportability and set-up. The blade could be designed into three sections of 12 ft each, with the two inboard sections all being constant chord. The criterion for spacing of the ribs is unknown and will probably be a function of the ease of tensioning and heat shrinking the Mylar. The spacing will most likely have to be determined after materials can be obtained

and a test section constructed. Adhering the film to the ribs can be easily done using a spray glue made by 3M called Spray 77 [Ref.33].

The support structure for the pilot, termed the "undercarriage," should also be made from composite tubing for maximum strength-to-weight ratio. The undercarriage includes the "landing gear" structure that provides some degree of protection by absorbing energy during landings and a means for the aircraft to stand upright.

The mast and rotor blade hubs shall also be fabricated from composites. Bearing races can be fabricated in the NPS workshops form metal. The hollow mast will allow control tubes/cables to pass through to the upper rotor blades. A scheme to allow pilot azimuthal control of the winglets for lateral/ longitudinal control needs to be devised in future design refinements.

D. DRIVE TRAIN

1. Chain/crank system

Past histories of human-powered aircraft have shown the drive train to be a neglected yet crucial element in the design and development of human-powered aircraft. Conversations with builders of two human-powered helicopters have confirmed this conclusion [Ref. 33 and 39]. The characteristics of a successful HPH drive system are

reliability, light weight , ability to withstand high torques, and simplicity.

Human power studies have shown pedalling to be the preferred method for this application. Hence, standard bicycle components should be used as they have several distinct advantages:

- They are proven to work as intended.
- They come in standard sizes and are easily interchangeable to obtain the optimum system.
- They could most likely be obtained gratis; either from local shops or the manufacturers.
- They can easily be modified (drilled out) to be made lighter.
- Many cyclists (potential pilots!) prefer certain gear (pedals for example) and can be easily interchange their own gear.
- Chain wheels can be easily changed to alter the main rotor drive gear ratio.

Further work on the ergometer may offer more information regarding the optimum crank system. In reality it will most likely be the pilot's choice/preference. The choice to use conventional bicycle components will offer advantages over custom designed equipment and should be considered.

The chain will be required to twist 90 degrees to operate in the same plane as the rotor shaft. A flexible chain is commercially available [Ref.40: p.A80] which is particularly suitable. Called POW-R-CHAIN, it has a 1/2 inch pitch and is compatable with standard bicycle drive gears. Made of

polyester rollers fixed to wire cables, it has a tensile strength of 300 lb and weighs only 1 ounce per foot.

Large torques are required on start-up, and a drive system is required to be able to withstand these large forces. The proposed bicycle crank/chain drive system is proven, simple and lightweight. The only disadvantage of a chain-drive system is the requirement for feeder slots for the chain going onto the gear.

2. Reversing Mechanism

Again, a robust drive system that is simple and lightweight is desired. The proposed reversing mechanism effectively combines these elements. A drawing of the reversing mechanism is presented in Figure H-1, Appendix H.

The rotor mast is centered about a main, stationary mast to which the undercarriage is fixed. Around this mast are two identical sleeves each of which serve as the rotor hub. Where the two sleeves meet, they are interconnected by an idler wheel. As the bottom sleeve rotates, the idler wheel will turn the upper sleeve at the same speed, except in the opposite direction. A bevelled pinion gear and ring gear will effectively accomplish the intended job. Available from commercial sources, they will have to be sized upon completion of the exact drive train design.

E. SUMMARY OF FINAL DESIGN

A summary of the design, dimensions and aircraft parameters is presented below:

COMPLETE HELICOPTER

Rotor diameter - 72 ft

Number of blades - 4

Total thrust - 250 lb

Rotor speed - 8 rpm

Planform area - 552 sq ft

Co-efficient of thrust (C_T) - .0206

ROTOR BLADES

Root chord - 4.5 ft (to 0.67R)

Tip chord - 2.5 ft

Taper ratio - 1.8

Tip speed - 30.5 fps

Tip loss factor - 9.65

Airfoil - DAI 11

POWER

Hp required at 3 meters (no ground effect) - 1.68 hp

Hp required at 3 meters (ground effect) - 1.30 hp

Hp required at low hover (ground effect) - 0.8 hp

Power loading (low hover) - 312.5 lb/hp

Pilot pedal speed - 90 rpm

A comparison of several rotor parameters is made with several other human-powered aircraft below:

TIP SPEED

This design - 30.5 ft/sec

Da Vinci - 55 ft/sec

Daedalus - 22 ft/sec

WING LOADING

This design - 0.453 lb/sq ft

Gossamer Condor - 0.25 lb/sq ft

Da Vinci III - 0.625 lb/sq ft

Musculair II - 1.4 lb/sq ft

Drawings of the HPH are presented in Appendix H.

VI. CONCLUSIONS AND RECOMMENDATIONS

A. BENEFITS OF AN HPH PROGRAM

This paper concludes that a 72-ft diameter co-axial helicopter can be hovered for one minute on human power. The construction of a human-powered helicopter and completion of a one minute hover to win the Igor I. Sikorsky Competition is well within the capabilities of students at the NPS. Construction of a human-powered helicopter at the NPS will have many benefits to the school, aeronautical engineering, naval aviation, and the Navy in general.

Winning the American Helicopter Society's competition will represent a historically significant milestone. As the last of Leonardo Da Vinci's ideas to be realized, winning the Igor I. Sikorsky Human-Powered Helicopter Award will be an achievement that will assure the school a great deal of prestige within the aviation and engineering community. The publicity generated from a successful flight will present a very positive image for the NPS and the Navy in general.

In addition to the intangible rewards, there will be many very real and positive benefits with respect to the Aeronautical Engineering curriculum. One of the most needed benefits of a program such as this will be the promotion of the helicopter aerodynamics program at the NPS. The NPS has

probably the best body of helicopter knowledge of any educational institution in the world. Approximately one-third of the aeronautical engineering students are helicopter pilots. These pilots include graduates of the U.S. Naval Test Pilot School, undoubtedly the best helicopter test pilot school in the world; pilots with several thousand helicopter flight hours; pilots with significant fixed-wing hours as well as rotary-wing hours; and pilots who were prior aircraft maintainers. Also included as students are government service and foreign engineers who are helicopter specialists. With such an outstanding indigenous body of knowledge, the NPS should be one of the leading helicopter research institutions in the world.

The U.S. Army sponsors three universities within the U.S. to conduct helicopter research. Called "Army Rotorcraft Centers of Excellence," these universities include University of Maryland, Rensselear Polytechnic Institute, and Georgia Institute of Technology.[Ref.41: p.56] The Navy should endeavor to make the NPS a similar facility for conducting helicopter research for naval-related issues.

With all of the composite parts of the HPH, a program to build an HPH will enhance the composite program and facilities at the NPS. There is a very real need to educate naval aeronautical engineers on advanced composite technology. Naval aircraft of the future, such as the V-22 and the A-X, will have significant portions of the airframe and associated

components fabricated from composite materials. The school already has considerably less well equipped composite facilities than other top-scale aeronautical engineering universities in the U.S.

B. FLIGHT TEST OPPORTUNITIES

Given the nature of the body of helicopter knowledge at the NPS, the particular strong point is flying knowledge and experience. A simple aircraft such as an HPH would allow some simple flight test opportunities without the tremendous difficulties involved in flying military aircraft. The HPH can be motorized and hover-power measured accurately for performance testing. A flight test course is currently taught within the department, and the aircraft would be an ideal platform for use in that course. Some of the flight test subjects possible for an HPH are presented in the following subsections:

1. Highly flexible aircraft

Conventional aerodynamics assumes a rigid body; however, airframes are non-rigid and airframe flexure affects aircraft dynamic responses. Flight testing of highly flexible fixed-testing of the Light Eagle that parameter estimation and computational modeling became much more difficult and complicated than was previously thought [Ref.42: p.349].

2. Instrumentation research

Developing ultra-light inflight instrumentation for the HPH could lead to further developments for flight test or operational use. The F-18 operational in-flight airframe-stress-monitoring-system was an NPS by-product and is an example of the type of instrumentation program that might originate from instrumentation research on the HPH.

3. Flying Qualities

The HPH can be used as vehicle to teach and study flying qualities. An understanding of the terms, influences and variables concerning flying qualities is important for all pilots.

4. Simulation

In this era of budget tightening, flight time will become increasingly scarce. As a result, an increased emphasis will be placed on simulation with respect to earning and maintaining fleet qualifications. Just as it is important for fleet aviators to know about real aircraft and aircraft systems, so it is important to know about simulation and simulators. Creation of a HPH simulator will be a means for learning and applying those principles. An interdiscipline subject, simulation incorporates everything from flight test data to control systems to basic aerodynamics, and creates an excellent learning and research opportunity.

REFERENCES

1. Drela, M. and Langford, J., "Human-powered Flight," Scientific American, June 1988.

2. Burke, J. D., The Gossamer Condor and Albatross: A Case Study in Aircraft Design," AIAA Professional Study Series, Report No. AV-R-80/540, 16 June 1980.

3. Patterson, W.B., "The Leonardo Da Vinci Flies! A Very Brief Overview of the First Human Powered Hover," Vertiflite, Mar/Apr 1990.

4. Dorsey, G., The Fullness of Wings,1st ed., Viking Penguin, 1990.

5. Whitt, F.W. and Wilson, D.G., Bicycle Science, 2nd ed., Cambridge Press, 1982.

6. Gay, R.R., "The Frame on the Frame," Bike Tech, April 1988.

7. Okajima, S.,"RPM Versus Power," Cycling Science, September, 1990.

8. Drela, M., "Aerodynamics of Human Powered Flight," AnnualReview of Fluid Mechanics, Annual Review Inc., 1990.

9. Grohsmeyer S, and others, A Design for a Human-Powered Helicopter, AE 4306 Class Presentation, Naval Postgraduate School, Monterey, Ca., 1990.

10. Pfenninger, W. and Vemru, C.S., "Design of Low Reynolds Number Airfoils: Part I," Journal of Aircraft, vol.27, no.3, March 1990.

11. Marchman, J.F., "Aerodynamic Testing at Low Reynolds Numbers," Journal of Aircraft, vol.24, no.2, February 1987.

12. Drela, M., "Low Reynolds Number Airfoil Design for the M.I.T. Daedalus Prototype: A Case Study," Journal of Aircraft, vol.25, no.8, August 1988.

13. Mueller,T.J., "The Influence of Laminar Separation and Transition on Low Reynolds Number Airfoil Hysteresis," Journal of Aircraft, vol.22, no.9, Sep 85.

14. Howard, R.M. and Kindelspire, D.W., "Freestream Turbulence Effects on Airfoil Boundary Layer Behavior at Low Reynolds Numbers," Journal of Aircraft, vol.27, no.25, May 90.

15. Howard, R.M. and Renoud, R.W., "Wing Boundary Layer Response to an Unsteady Turbulent Flowfield," Journal of Aircraft, to be Published.

16. Selig, M.S., Donovan, J.F., and Fraser, D.B., Airfoils at Low Speeds, 1st ed., H.A. Stokeley, 1989.

17. U.S. Department of Energy, A Catalog of Low Reynolds Number Airfoil Data For Wind Turbine Applications, Miley, S.J., Government Printing Office, Washington D.C., 1982.

18. Letter from P.B.S. Lissaman, Aerovironment Inc., to author, 24 Oct, 90.

19. Telephone conversation between Prof. Mark Drela, M.I.T., and the author, 16 Apr 1991.

20. Facsimile from Prof. Mark Drela, M.I.T., to the author, 16 Apr 1991.

21. Gessow, A. and Myers, G.C., Aerodynamics of the Helicopter, Fredrick Ungar, 8th printing, 1985.

22. Prouty, R.W., Helicopter Performance, Stability and Control, Robert E. Krieger, 1990.

23. U.S. Army Transportation Research Command, Parametric Investigation of the Aerodynamic and Aeroelastic Characteristics of Articulated and Rigid (Hingeless) Helicopter Rotors Systems, Trecom technical report 64-15, April 1964.

24. Johnson, W., Helicopter Theory, pp. 59-60, Princeton Press, 1980.

25. Peters, D.A. and Chiu, Y.D.,"Extension of Classical Tip loss Formulas," AHS Journal,5, pp.68-71, April 1989.

26. Bertin, J.J., and Smith, M.L., Aerodynamics for Engineers, 1st ed., Prentice Hall, 1979.

27. Nakamura, S., Applied Numerical Methods With Software, 1st ed., Prentice-Hall, 1991.

28. Wood, E.R., and Hermes, M.E., Rotor Induced Velocities inForward Flight by Momentum Method, AIAA paper no. 69-224

29. Anderson, J.D., Fundamentals of Aerodynamics, 1st ed., McGraw-Hill, 1984.

30. Prouty, R.W., "Ground Effect In Hover," Rotor and Wing, February, 1991.

31. Daughaday, H. and Parrag, M.L., Helicopter Stability and Contro Theory and Flight Test Techniques, Preliminary Draft, CALSPAN report no.6645-F-10, 1983.

32. Telephone converstion between Mr. P. Zwann, AeroVironment Inc., and the author, October, 1990.

33. Judge, J.F., "Composite Materials: The coming Revolution, Airline Management and Marketing, September, 1969.

34. National Aeronautics and Space Administration, NASA Conference Publication 3104 Pt. 2, "Comparison of Hand Laid-up tape and Filament Wound Composite Cylinders and Panels With and Without Impact Damage," First NASA Advanced Composites Technology Conference, Jegley and Lopez, 1991.

35. Jones, R.M., Mechanics of Composite Materials, 1st ed., Hemisphere Publishing, 1975.

36. Marshall, A.C., Composite Basics, 2nd ed., Marshall Consulting, 1989.

37. Aircraft Spruce and Specialt Company Catalog, Box 424 Fullerton, Ca, 1990.

38. Telephone conversation between Mr. W. Petterson, Cal Poly San Luis Obispo, and the author, October 1990.

39. Berg Precision Mechanical Components Catalog, Winfred M. Berg Inc. 499 Ocean Ave., East Rockaway, NY 11518, B8.

40. Singleton, R.E., "Army Conference Highlights Rotorcraft Centers of Excellence," Vertiflite, Mar/Apr 1991.

41. Zerweckh, S.H., and Von Flowtow, A.H., "Flight Testing A Highly Flexible Aircraft: Case Study on the MIT Light Eagle, Journal of Aircraft, vol.27 no.4, Apr 90.

42. Lecture by Dr. Paul B. MacCready given as part of the Chevron Research and Technology Distinguished Speakers Series, 16 May, 1991, Richmond, Ca.

APPENDIX A:FIGURES

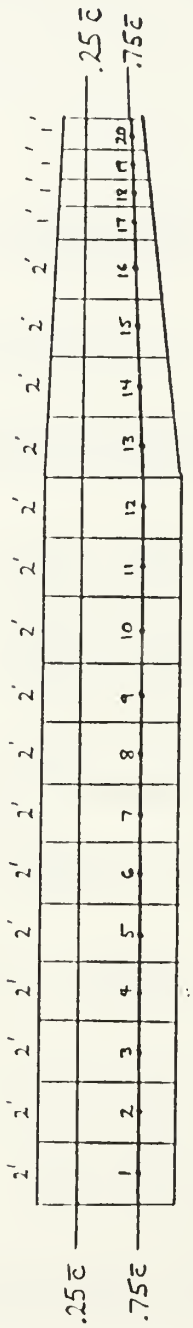

Figure A-1. ROTOR BLADE VORTEX DISTRIBUTION.

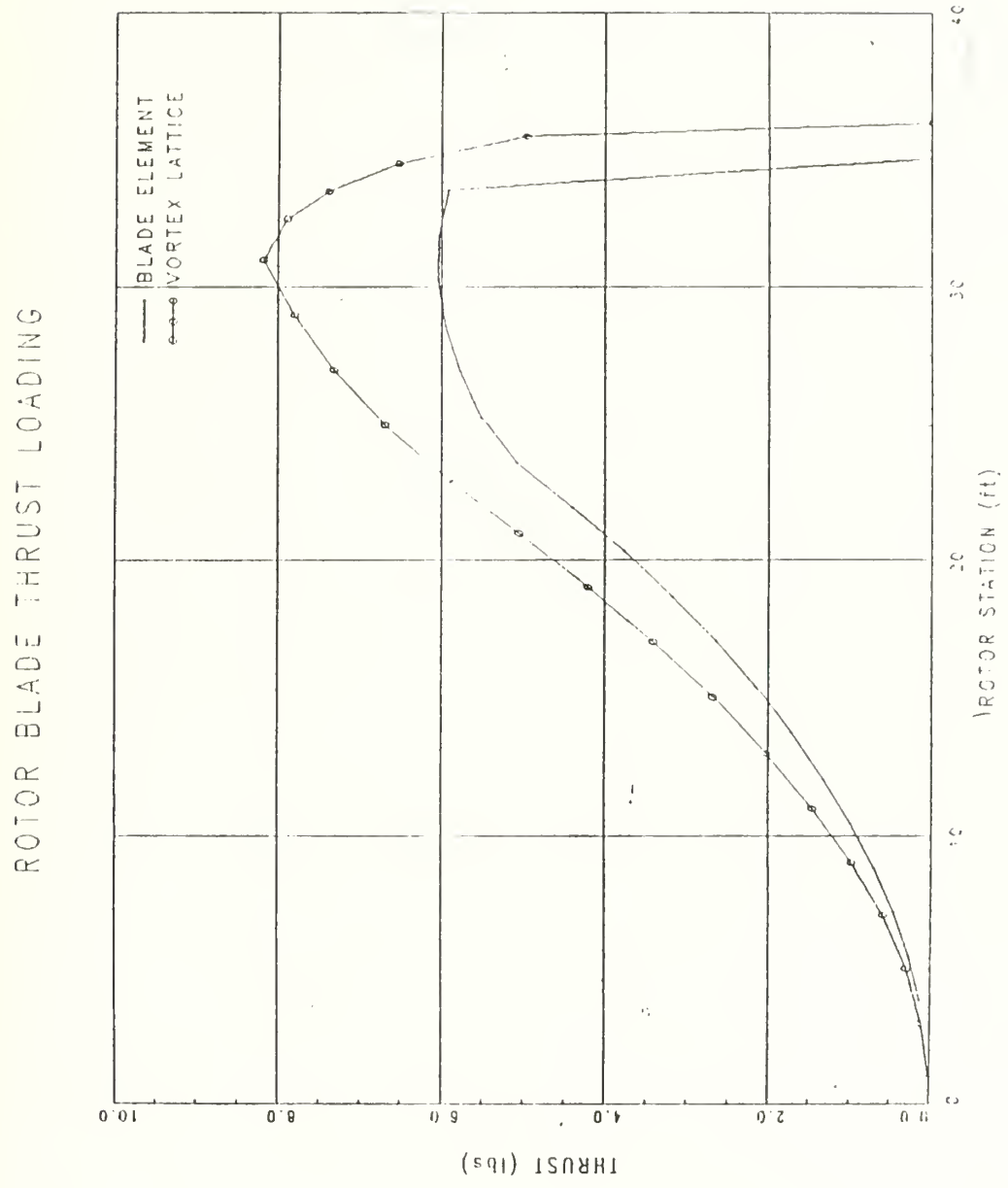

Figure A-2. ROTOR BLADE THRUST LOADING.

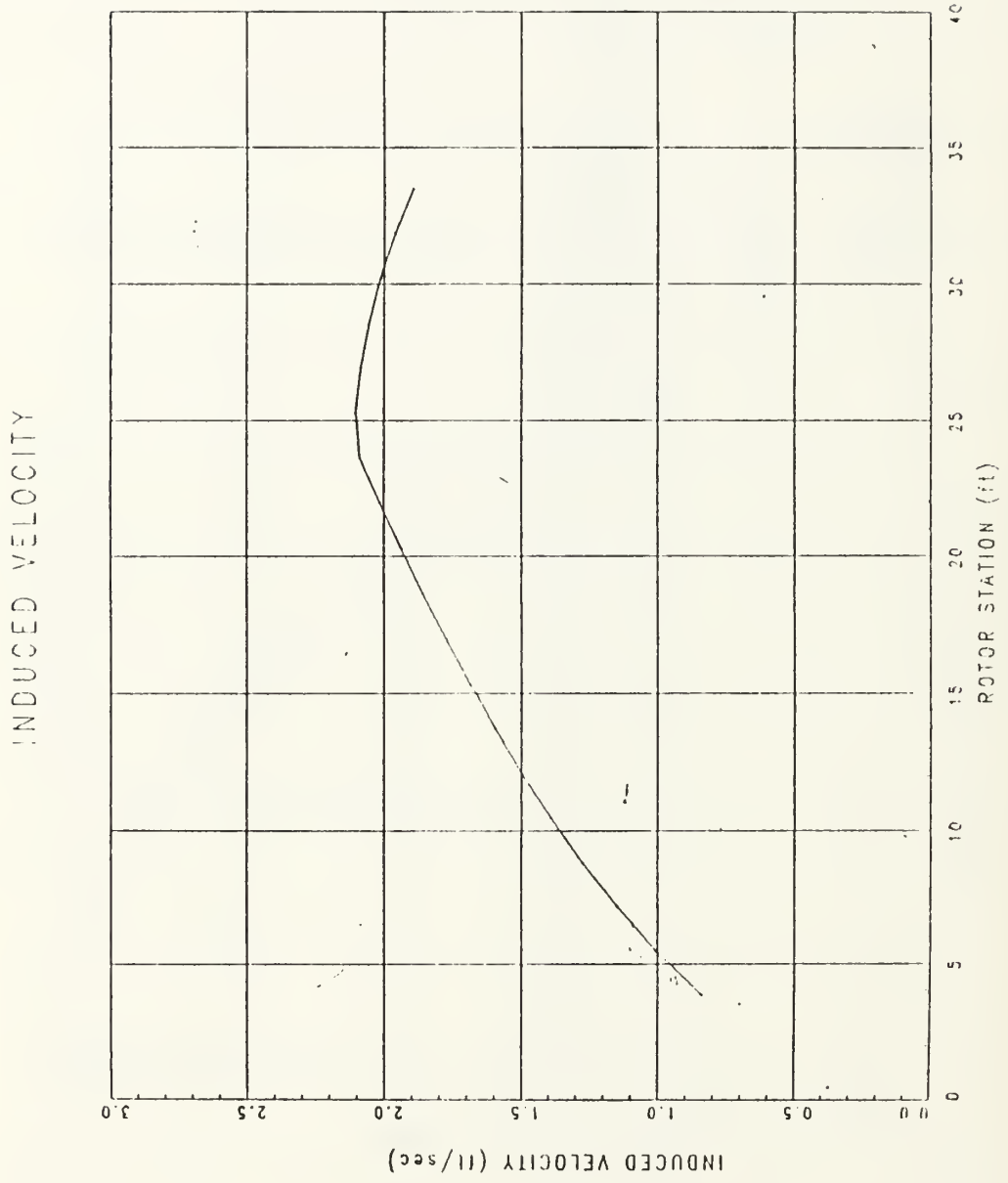

Figure A-3. ROTOR BLADE INDUCED VELOCITY.

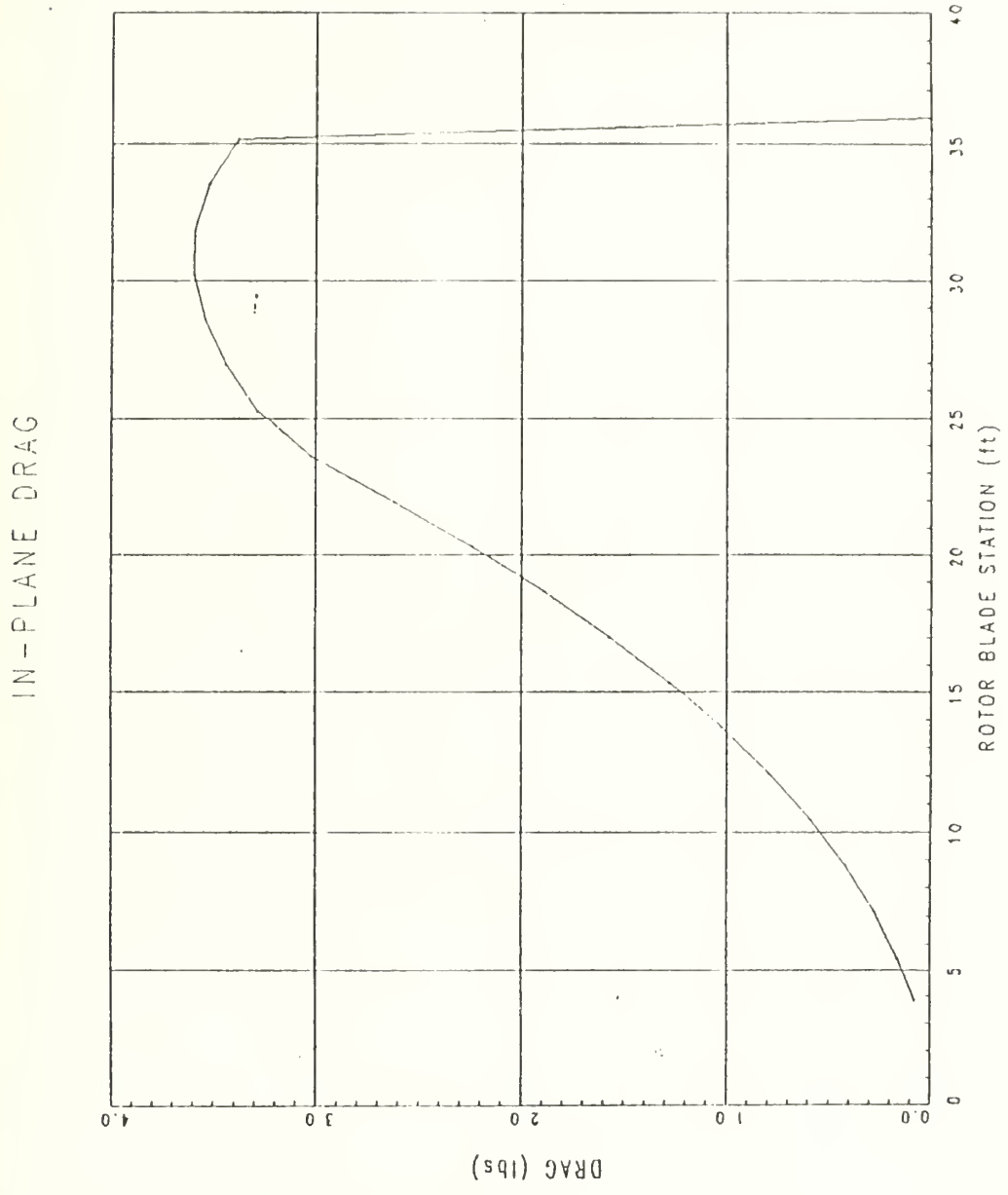

Figure A-4. ROTOR BLADE IN-PLANE DRAG.

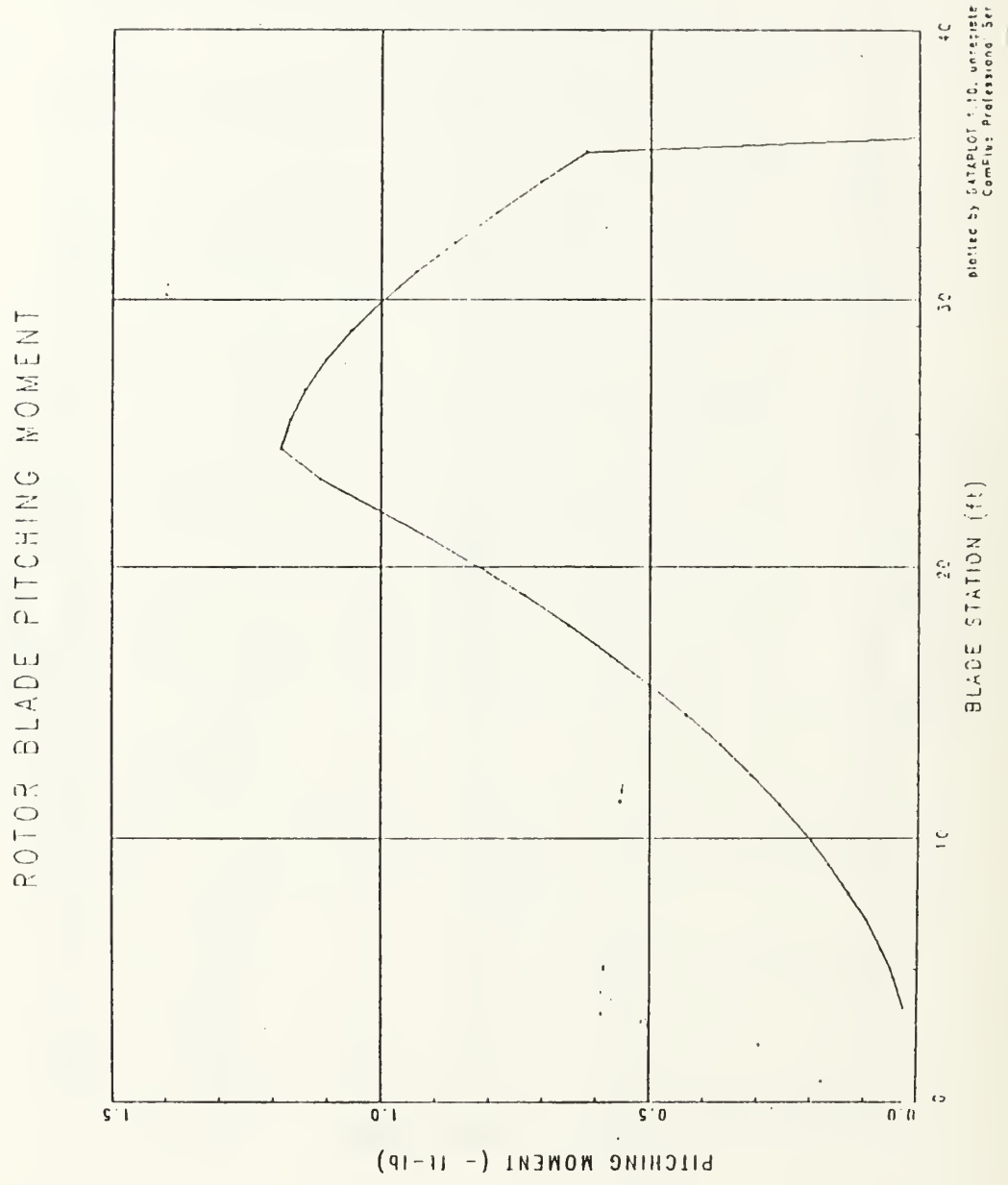

Figure A-5. ROTOR BLADE PITCHING MOMENT.

APPENDIX B: TABLES

BLADE STATION (ft)	CHORD (ft)	REYNOLDS NUMBER	INDUCED VELOCITY (ft/sec)
3.32500005	4.5	93,587	0.84087288
5.17499990	4.5	133,958	1.00602007
7.12500000	4.5	174,329	1.14764357
8.97499962	4.5	214,700	1.27361500
10.82500020	4.5	255,071	1.38820195
12.67499980	4.5	295,442	1.49402618
14.52499940	4.5	335,813	1.59283495
16.37500000	4.5	376,184	1.68586266
18.22499960	4.5	416,554	1.77401865
20.07499920	4.5	456,925	1.85799658
21.92499890	4.5	497,296	1.93833959
23.77500040	4.5	537,667	2.01548266
25.62500000	4.5	578,038	2.08977985
27.47499960	4.27	586,344	2.10473919
29.32499920	3.93	575,823	2.08577085
31.17499890	3.60	559,321	2.05566692
33.02500040	3.27	536,838	2.01392794
34.87500000	2.93	508,375	1.95981097
36.72499770	2.60	473,930	1.89225423

Table B-1. ROTOR BLADE STATION REYNOLDS NUMBERS.

ROTOR STATION (FT)	CIRCULATION (sq ft/sec)
1.00000000	1.53017879
3.00000000	4.58750963
5.00000000	7.63552904
7.00000000	10.66722390
9.00000000	13.67425540
11.00000000	16.64608000
13.00000000	19.56073700
15.00000000	22.42279050
17.00000000	25.17988970
19.00000000	27.79636190
21.00000000	30.19985960
23.00000000	32.25499730
25.00000000	33.59384540
27.00000000	34.03530510
29.00000000	33.75513460
31.00000000	33.12871550
32.50000000	30.47932240
33.50000000	27.64979930
34.50000000	23.81584930
35.50000000	17.36374090

BLADE STATION (ft)	THRUST (lb)	DRAG (lb)
2.82500005	0.13327463	0.07933248
5.47499990	0.27305669	0.16253854
7.12500000	0.46243888	0.27526936
8.77499962	0.70142114	0.41752487
10.42500020	0.99000359	0.58930522
12.07499980	1.32818604	0.79061025
13.72499940	1.71596837	1.02143991
15.37500000	2.15335131	1.28179455
17.02499960	2.64033365	1.57167363
18.67499920	3.17691660	1.89107752
20.32499890	3.76309896	2.24000597
21.97500040	4.39888239	2.61845970
23.62500000	5.08426619	3.02643824
25.27499960	5.51751041	3.28432918
26.92499920	5.77223825	3.43595767
28.57499890	5.95041323	3.54201698
30.22500040	6.04101038	3.59594560
31.87500000	6.03300858	3.59118247
33.52499770	5.91538620	3.52116704

Table B-2. ROTOR BLADE STATION CIRCULATION.

APPENDIX C: HPH COMPETITION RULES

American Helicopter Society

Igor I. Sikorsky

Human Powered Helicopter Competition

A prize of $20,000 is offered by the American Helicopter Society for a successful controlled flight of a human powered helicopter.

This competition shall be conducted under the following regulations and conditions laid down by the Human Powered Helicopter Committee of the American Helicopter Society, and shall be witnessed by the National Aero Club (NAC) who is the national representative of the Federation Aeronautique Internationale (FAI). In the United States, the national representative of the FAI is the National Aeronautic Association (NAA).

Note: The AHS has been advised by the Federal Aviation Administration (FAA) that, in the United States of America, registration and airworthiness certification will not be required for machines built for this competition on the assumption that all flights will be limited to close proximity to the ground and will generate no interference with air commerce. All intending entrants are strongly advised, during trials, to hold adequate insurance coverage for all third party risks and to take every precaution against injury to people and damage to property. It is expected that competitors in countries other than the U.S.A. will observe their own national flying and insurance regulations.

REGULATIONS

1. GENERAL

   1.1 The prize will be awarded by the AHS to the entrant who first fulfills the conditions.

   1.2 Additionally, an attempt will be registered with the Federation Aeronautique Internationale (FAI) as a World Record for Human-Powered Helicopter Flight duration.

2. PRIZE

   2.1 The AHS prize is $20,000 in U.S. currency.

3. ELIGIBILITY

3.1 The competition is international and is open to individuals or teams from any part of the world.

3.2 For any and all questions regarding the acceptance of entries, eligibility of an entrant, pilot, crew or aircraft under the regulations, or any other matter relating to the AHS prize, the decision of the AHS is final.

3.3 All questions regarding the world record attempt will be governed by the sporting code of the FAI and rest exclusively with the NAC.

4. CONDITIONS OF ENTRY

4.1 Aircraft

4.1.1 The machine shall be a heavier-than-air machine. The use of lighter-than-air gases shall be prohibited.

4.1.2 The machine shall be a rotary wing configuration capable of vertical takeoff and landing in still air, and at least one member of the crew shall be non-rotating.

4.1.3 The machine shall be powered and controlled by the crew during the entire flight, including accelerating the rotor up to takeoff speed.

4.1.4 No devices for storing energy either for takeoff or for use in flight shall be permitted. Rotating aerodynamic components, such as rotor blades, used for lift and/or control are exempt from consideration as energy storing devices.

4.1.5 No part of the machine shall be jettisoned during the flight including the rotor spin-up and takeoff.

4.2 Crew

4.2.1 The crew shall be those persons in the machine during takeoff and flight, and there shall be no limit set to their number.

4.2.2 No member of the crew shall be permitted to leave or enter the aircraft at any time during takeoff or flight.

4.2.3 No drugs or stimulants shall be used by any member of the crew. An assurance must be given to the official observers at the time of the attempt that this requirement has been met.

4.2.4 Up to two handlers or ground crew shall be permitted to assist in stabilizing the machine during takeoff and landing, but in such a manner that they do not assist in accelerating or decelerating any part of the machine.

4.3 Ground Conditions

4.3.1 All attempts, which shall include the takeoff, shall be made over approximately level ground (i.e., with a slope not exceeding 1 in 100 in any direction).

4.3.2 All attempts shall be made in still air, which shall be defined as a wind not exceeding a mean speed of approximately one meter per second (3.1 kilometers per hour, 2.237 statute miles per hour, 1.5 nautical miles per hour) over the period of the flight.

4.4 Flight Requirements

4.4.1 The flight requirements shall consist of hovering for one minute while maintaining flight within a 10-meter square. During this time the lowest part of the machine shall exceed momentarily 3 meters above the ground.

4.4.2 The machine shall be in continuous flight from takeoff to landing, and at no time during the flight shall any part of the machine touch the ground.

4.4.3 A reference point on the non-rotating part of the machine will be established as a means whereby the observers can judge that the machine stayed within the confines of the 10-meter square.

4.4.4 The one minute hovering time and the momentary achievement of 3 meters altitude is required to win the AHS prize. (However, the FAI 1980 regulations specify that only the duration of the flight and a momentary achievement of 3 meters altitude will be recorded for the FAI world record attempt, making it possible to achieve a world record without satisfying the AHS prize requirements.)

4.5 Observation

Every attempt shall be observed by the NAC or by any persons authorized by them to act as observers. It may take place in the competitor's own country if it is affiliated with the FAI. In a country not so, it could be advantageous to conduct the flight in a neighboring country which is so affiliated.

5. APPLICATIONS FOR ENTRY

5.1 Entry forms shall be obtained from and returned to the American Helicopter Society, 217 North Washington Street, Alexandria, VA 22314, (703)684-6777.

5.2 The entry fee shall be U.S. $15 (made payable to the American Helicopter Society).

5.3 Each entry form shall contain an application for official observation of the competitor's attempt.

5.4 The entrant shall undertake to abide by the conditions for official observation as set out on the entry form and application for official observation and shall undertake to defray all expenses incurred in connection with the official observation of the attempt.

5.5 The following fees and charges are made by the NAA for record attempts in Class I, Human Powered Aircraft. All attempts shall be for national and international records.

5.6 Final notice of the proposed time and place of the attempt requiring official observation may, if so desired, be sent to the AHS later than the entry form. It must in all cases be received at least thirty days before the proposed date for the attempt. This time is required by the NAC (the NAA in the U.S.A.) to arrange for official observation. Applications will be considered in order of receipt.

5.7 Membership in the appropriate NAC and an FAI Sporting License is required for all crew members taking part in this competition. Application forms may be obtained from the NAC of the AHS. For this competition, a pilot's license is not required.

6: GENERAL CONDITIONS

6.1 Insurance

The entrant must take out on behalf of himself, his crew, representatives or employees, liability insurance in such form and mount to be specified by the AHS, to indemnify the American Helicopter Society, the NAC and the FAI against any claims. Evidence that such insurance has been effected must be submitted with the application for official observation.

6.2 Revision of Regulations

6.2.1 These regulations shall remain in force until such time as the AHS considers it necessary to amend them, or the prize has been won.

6.2.2 The AHS reserves the right to add to, amend or omit any of these regulations and to issue supplementary regulations.

6.3 Interpretation of Regulations

The interpretation of these regulations or any of the regulations hereafter issued rest entirely with the AHS. The entrant shall be solely responsible to the official observer for due observance of these regulations and shall be the person with whom the official observers will deal in respect thereof, or any other questions arising out of this competition.

APPENDIX D: ERGOMETER

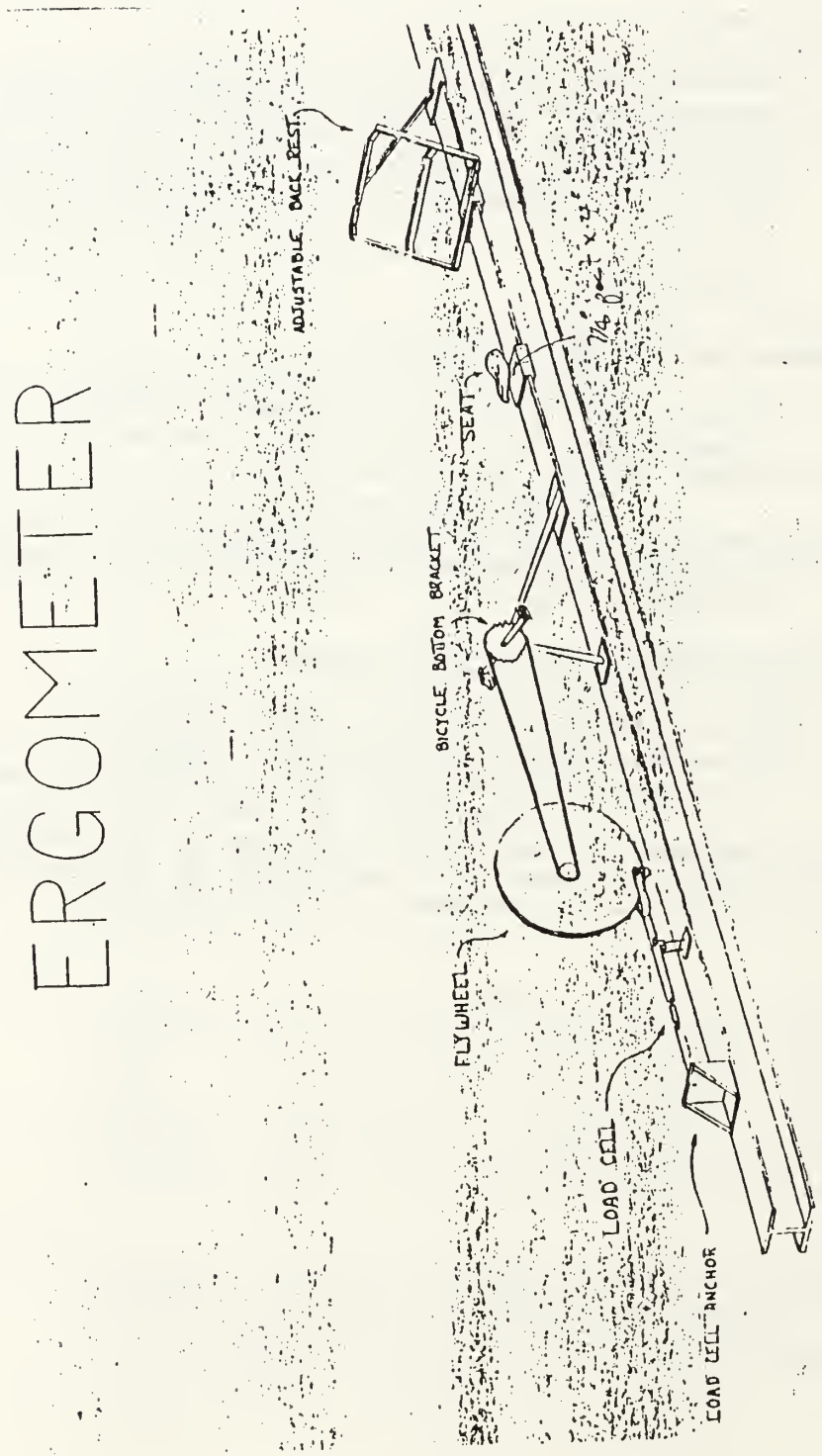

interface SEALED SUPER-MINI LOAD CELLS

ADVANCED FORCE MEASUREMENT

Model SSM-100

Designed for Precision Electronic Force Measurement

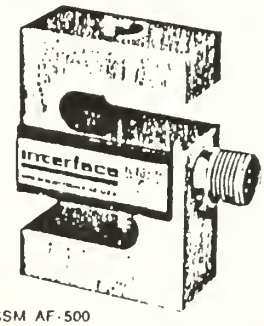

Model SSM-AF-500

FEATURES

- Ultra Precision
- Excellent Linearity
- High Repeatability
- Thermally Compensated
- Low Moment Sensitivity
- Low Cost
- Easily Installed
- NBS Handbook 44 Sealable

RATED CAPACITIES: 50, 100, 250, 500, 750, 1000, 2000, 3000, and 5000 pounds
(222N, 445N, 1112N, 2224N, 3336N, 4448N, 8896N, 13345N, 22241N)

The Sealed Super-Mini load cell is a precision strain gage load cell which is waterproof and barometrically insensitive. It is designed for testing, weighing & force measurements in tension & compression. Interface's application of proprietary advanced materials technology, in strain gage and flexure design, produces load cells with the highest accuracy in the industry yet priced competitively with lower performance units.

These rugged cells have no moving parts to wear out or get out of adjustment. The specifications listed below illustrate the superior performance of Interface Sealed SSM Series load cells and are a major factor in their worldwide acceptance in applications such as structural force testing, thrust measurement, steelyard rod conversions (to H-44, and OIML requirements), conveyor scales, check weighers, counting and white scales, tensile testing and engine dynamometers.

For metric applications see Metric Sealed Super Mini Series offering 500N, 1000N, 2000N, and 5000N capacities and metric mounting threads.

For applications not requiring waterproof sealed units, see the Super-Mini series of load cells with Moisture Resistant (MR) coating.

SPECIFICATIONS[1]

Non-Linearity—% Rated Output	± 0.05
Hysteresis—% Rated Output	± 0.03
Non-Repeatability—% Rated Output	± 0.02
Temperature Range, Compensated—°F (–15° to 65°C)	0 to 150
Temperature Range, Operating—°F (–55° to 90°C)	–65 to 200
Temperature Effect on Rated Output—% of Reading/100°F (% of Reading/55.6°C)	± 0.08
Temperature Effect on Zero—% Rated Output/100°F (% of Rated Output/55.6°C)	± 0.15
Creep, After 20 Min.—% Rated Output[2]	± 0.03
Overload Ratings—% Rated Capacity	
Safe	± 150
Ultimate	± 500
Nominal Output—mV/V	3
Zero Balance—% Rated Output	± 1
Input Resistance—Ohms	350 + 50/ – 3.5
Output Resistance—Ohms	350 ± 3.5
Excitation Voltage	
Recommended—VDC	10
Insulation Resistance, Bridge to Case—Megohms	5000

(1) Per SMA "Load Cell Terminology and Definitions".
(2) Creep specification is determined at rated capacity. Creep performance at reduced loads is proportional to the applied load.

Copyright © 1985 by INTERFACE INC.

interface SEALED SUPER-MINI LOAD CELLS

SEALED SUPER-MINI LOAD CELLS

INSTALLATION DIMENSIONS

MODEL		A	B	C	D
SSM-50	Inch	2½	2	⅛	¼-28 UNF-2B
	mm	64	51	22	¼ deep, top & bottom
SSM-100, 250	Inch	2½	2	¾	¼-28 UNF-2B
	mm	64	51	19	¼ deep, top & bottom
SSM-500, 750,	Inch	3	2	1¼	½-20 UNF-2B
1000, 2000, 3000	mm	78	51	32	½ deep, top & bottom
SSM-5000	Inch	3½	2½	1¾	⅝-18 UNF-2B
	mm	89	64	44	⅝ deep, top & bottom

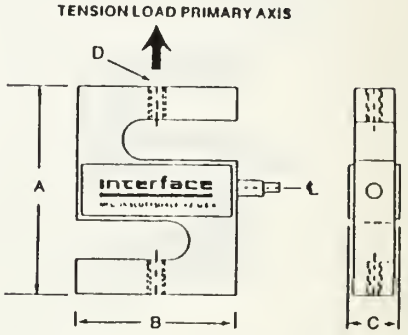

ELECTRICAL INFORMATION

The SSM-50 thru SSM-250 is supplied with a 4 conductor shielded cable (AWG28) 10 ft (3m) long. The SSM-500 thru SSM-5000 load cells are supplied with a rugged cable (PVC Jacket AWG22) 10 ft (3m) long or a Bendix PC04E-10-6P connector. A PC06W-10-6S mating connector is available at additional cost.

Connector (SSM-500 thru 5000)		Cable (All Models)	
Pin	Function	Color	Function
A	+ Excitation	Red	+ Excitation
B	+ Output	Green	+ Output
C	- Output	White	- Output
D	- Excitation	Black	- Excitation
E	No Connection	Shield	No Connection
F	No Connection		

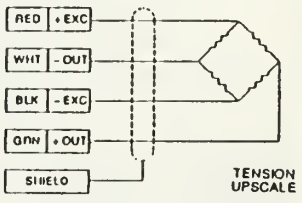

Wiring Code Complies with ISA S37.8 "Specification and Tests for Strain Gage Force Transducers" and SMA Load Cell Terminology.

APPLICATION NOTES

1. The Sealed Super-Mini load cell is specifically designed for outdoor usage and thus can be used in scale pits and batching plants or other locations that are directly exposed to the weather.
2. At least one diameter thread engagement is desirable; normal engagement is shown below:
   SSM-50 thru 250: ¼" (8mm) to ½" (12mm)
   SSM-500 thru 3000: ½" (12mm) to ⅝" (16mm)
   SSM-5000: ⅝" (16mm) to ¾" (19mm)
3. SSM-50 thru and including SSM-1000 are anodized aluminum. All other units are electroless nickel plated steel.

   Bottoming out of the mounting stud can cause irreparable damage to the load cell.
4. Jam nuts may be used; however, care should be exercised to limit the installation torque as follows:

SSM-50:	20 inch pounds	(2.2N-m)
SSM-100 thru SSM-250:	40 inch pounds	(4.5N-m)
SSM-500 thru SSM-1000:	200 inch pounds	(22.5N-m)
SSM-2000 and SSM-3000:	800 inch pounds	(90N-m)
SSM-5000:	1000 inch pounds	(113N-m)

5. The force to be measured should be applied to the active end of the cell to eliminate possible errors due to cable interaction. The active end of the cell is seperated from the cable/connector side by the slot (cutout) in the flexure (the serial number is always shown on the inactive side.)

TERMS AND CONDITIONS

1. *Ordering Information*: Sealed Super-Minis are ordered by specifying Series (SSM), Model (AJ for cable or AF for connector) and capacity (50 through 5000 lbs.) *Example*: SSM-AJ-250 or SSM-AF-1000.
2. *Pricing*: Consult your local Interface Representative or the factory for price and delivery.
3. *Terms*: Net 30 days in U.S. dollars, FOB Scottsdale, Arizona U.S.A.
4. *Warranty*: Interface, Inc. 's standard two-year warranty is applicable to the Sealed Super-Mini Series load cell. Interface, Inc. certifies that its calibration measurements are traceable to the U.S. National Bureau of Standards (NBS).

Prices and specifications subject to change without notice.

interface
ADVANCED FORCE MEASUREMENT
INTERFACE, INC. • 7401 E. BUTHERUS DR. • SCOTTSDALE, ARIZONA 85260 USA • (602) 948-5555 • TELEX: 325-382
15-27L 787 9K
Printed in U.S.A.

```
00003 C     THIS PROGRAM WILL COMPUTE THE LIFT FOR A FOUR BLADED
00004 C     HELICOPTER USING BLADE ELEMENT THEORY
00005 C     THE PROGRAM USES A LINEAR TAPER FOR THE OUTBOARD 33%
00006
00007       REAL B,C,R,RR,O,E,N,VI,A,X,DR,RE,V,OR,M,CT,CR,B1,B2,ID,TC
00008       REAL L,TST,TS4,Q,QT,TS,IV,IVT,IVTA,CM,MT
00009       PRINT*,'INPUT ROTOR RADIUS IN FEET:'
00010       READ*,RR
00011
00012 C                          "E" IS THE OFFSET
00013       E=3
00014
00015       PRINT*,'INPUT THE ROOT CHORD AND TIP CHORD IN FEET:'
00016       READ*,CR,CT
00017
00018       PRINT*,'INPUT THE ROTOR RPM:'
00019       READ*,OR
00020       O=OR*3.1416/30
00021
00022 C                          "I" IS THE NUMBER OF BLADE ELEMENTS
00023       I=30.0
00024       I=I
00025       TST=0
00026 C                               Cl, Cd, & Cm ARE FOR DAE11 AIRFOIL
00027       CL=1.4506
00028       CD=0.01177
00029       CM=0.11
00030 C                          THESE VALUES ARE FOR 0 AOA-FOR FLAT PITCH
00031 C     CL=.5785
00032 C     CD=.01018
00033 C                          PHI IS INFLOW ANGLE AND IS EQUAL TO THE
00034 C                          BLADE ANGLE, 8 DEGREES FOR DAE11.
00035       PHI=8/57.3
00036
00037 C                          TO ACCOMODATE TIP LOSSES
00038       B1=1-CT/(2*RR)
00039       TC=250/(3.1416*RR**4*0.0023767*O)
00040       B2=1-SQRT(2*TC)/2
00041
00042 C                          "DR" IS THE LENGTH OF THE BLADE ELEMENT
00043       DR=(RR-E)/I
00044
00045 c     OPEN(10,FILE='THRUST.DAT',STATUS='NEW')
00046 c     OPEN(11,FILE='DRAG.DAT',STATUS='NEW')
00047 c     OPEN(12,FILE='REYNOLD.DAT',STATUS='NEW')
00048 c     OPEN(13,FILE='INDVEL.DAT',STATUS='NEW')
00049 c     OPEN(14,FILE='MOMENT.DAT',STATUS='NEW')
00050
00051         DO 100 N=1,I
00052           R=DR*N-DR/2+E
00053 C                          "M" IS THE SLOPE FOR THE EQUATION FOR CHORD
```

```
00054                ENDIF
00055
00056              V=R*O
00057              CALL REYNOLD (C,V,RE)
00058
00059              PRINT*,'CHORD IS:',C,'  R=',R,'  Re=',RE
00060              WRITE(12,*) C,R,RE
00061
00062              L=4*.5*.07646*(O*R)**2*CL*DR*C/32.17
00063              D=4*.5*.07646*(O*R)**2*CD*DR*C/32.17
00064
00065 C                          "TS" IS THE ELEMENTAL THRUST
00066              TS=L*COS(PHI)-D*SIN(PHI)
00067              TS4=TS/4
00068
00069            IF (R.GT.(B1*RR)) THEN
00070              TS4=0
00071              TS=0
00072            ENDIF
00073              WRITE(10,*) R,TS4
00074
00075 C                          "IV"=INDUCED VELOCITY
00076              IV=SQRT(TS4/(4*3.1415*.0023767*R*DR))
00077 C            PRINT*,'R=',R,'IND. VEL. =',IV
00078              WRITE(13,*)R,C,RE,IV
00079
00080 C                          "TST"IS THE TOTAL THRUST
00081
00082              TST=TST+TS
00083 C                          "ID"IS THE IN-PLANE DRAG
00084               ID=L*SIN(PHI)+D*COS(PHI)
00085               WRITE(11,*) R,ID
00086               Q=ID*R
00087               QT=QT+Q
00088
00089 100        CONTINUE
00090 200        CONTINUE
00091          CLOSE (10)
00092          CLOSE (11)
00093          CLOSE (12)
00094          CLOSE (13)
00095          VT=RR*O
00096          PRINT*,' '
00097          PRINT*,'THE TOTAL THRUST IN POUNDS IS:',TST
00098          HP=QT*O/550
00099          PRINT*,'THE TOTAL HORSEPOWER REQUIRED IS:',HP
00100          PRINT*,'THE TIP SPEED IS:',VT
00101          PRINT*,'THE TIP LOSSES (B1 AND B2) ARE',B1,B2
00102          END

NUMBER OF WARNINGS IN PROGRAM UNIT: 0
NUMBER OF ERRORS   IN PROGRAM UNIT: 0

00103          SUBROUTINE REYNOLD (C,V,RE)
```

```
00104        RL-6410^C^V
00105        END

NUMBER OF WARNINGS IN PROGRAM UNIT:  0
NUMBER OF ERRORS   IN PROGRAM UNIT:  0

NUMBER OF WARNINGS IN COMPILATION :  0
NUMBER OF ERRORS   IN COMPILATION :  0
```

```
00001 C          ******VORTEX LATTICE METHOD*****
00002
00003 C       THIS PROGRAM COMPUTES THE LIFT OVER A ROTOR BLADE
00004 C     USING THE VORTEX LATTICE METHOD WITH ONLY ONE CHORDWISE
00005 C     PANEL. THE COORDINATES OF THE PANELS AND CONTROL POINTS
00006 C     SET UP AS IN REF.22 p.271. TO MODIFY THE PROGRAM, THE PANEL
00007 C     COORDINATES NEED TO BE PUT INTO A FILE CALLED VLM2.DAT. THE
00008 C     ARRAY VARIABLES IN LINES 0001,0002,0010 AND 0092 NEED TO BE
00009 C     ADJUSTED TO THE NUMBER OF PANELS. THE PROGRAM USES THE VALUE
00010 C     OF AIR DENSITY FOR STANDARD DAY SEA LEVEL. THE VALUES FOR
00011 C     OMEGA, ROTOR DIAMETER, AND ANGLE OF ATTACK ARE NOT PROMPTED AND
00012 C     NEED TO BE ADJUSTED IN THE BODY OF THE PROGRAM. THE SUBROUTINE
00013 C     GAUSS IS MODIFIED FROM THE PROGRAM GIVEN IN REF.23 p.
00014 C     THE PROGRAM OUTPUTS TWO FILES: GAMMA.DAT WHICH IS A DATA FILE
00015 C     CONTAINING (IN ORDER) ROTOR BLADE STATION AND CIRCULATION, AND
00016 C     VLM3.DAT WHICH CONTAINS THE ROTOR BLADE STATION AND LIFT AT THE
00017 C     CONTROL POINT.
00018
00019       REAL X(20),Y(20),X1(20),X2(20),Y1(20),Y2(20),A
00020       REAL W1,W2,W3,W4,W5,W(20,21),W6,L(20),GAMMA(20)
00021       REAL OMEGA,B,ALPHA,LIFT
00022       OMEGA=.838
00023 C                              OMEGA=ROTOR SPEED IN RAD/SEC
00024       B=72
00025 C                              B=ROTOR DIAMETER
00026       ALPHA=.1396
00027 C                              ALPHA=ANGLE OF ATTACK IN RADIANS
00028       Z=20
00029 C                              Z= THE NUMBER OF PANELS
00030       OPEN(12,FILE='VLM2.DAT',STATUS='OLD')
00031          DO 200 I=1,Z
00032          READ(12,*)E,X(I),Y(I),X1(I),Y1(I),X2(I),Y2(I)
00033          PRINT*, E,X(I),Y(I)
00034 200      CONTINUE
00035       CLOSE(12)
00036 C                              VLM2.DAT CONTAINS THE LATTICE COORDINATES
00037 C                              X(I),Y(I) ARE THE COORDINATES OF THE CONTROL
00038 C                                                          POINTS.
00039 C                              X1(I),Y1(I) ARE THE LEFT HAND CORNERS OF THE
00040 C                                                    HORSESHOE VORTICES.
00041 C                              X2(I),Y2(I) ARE THE RIGHT HAND CORNERS OF THE
00042 C                                                    HORSESHOE VORTICES.
00043 100    CONTINUE
00044
00045       DO 400 M=1,Z
00046          DO 300 N=1,Z
00047
00048          W1=1/((X(M)-X1(N))*(Y(M)-Y2(N))-(X(M)-X2(N))*(Y(M)-Y1(N)))
00049
00050          W2=((X2(N)-X1(N))*(X(M)-X1(N))+(Y2(N)-Y1(N))*(Y(M)-Y1(N)))/
00051      &      (((X(M)-X1(N))**2+(Y(M)-Y1(N))**2)**0.5)
00052
00053          W3=((X2(N)-X1(N))*(X(M)-X2(N))+(Y2(N)-Y1(N))*(Y(M)-Y2(N)))/
```

```
00054      &        (((X(M)-X2(N))**2+(Y(M)-Y2(N))**2)**0.5)
00055
00056            W4=(1/(Y1(N)-Y(M)))*(1+(X(M)-X1(N))/((X(M)-X1(N))**2
00057      &        +(Y(M)-Y1(N))**2)**0.5)
00058
00059            W5=(1/(Y2(N)-Y(M)))*(1+(X(M)-X2(N))/(((X(M)-X2(N))**2
00060      &        +(Y(M)-Y2(N))**2)**0.5))
00061
00062            W6=W1*(W2-W3)+W4-W5
00063            IF (Q.EQ.2) W6=-W6
00064            W(M,N)=W(M,N)+W6
00065  300       CONTINUE
00066  400    CONTINUE
00067
00068          IF (Q.EQ.2) GO TO 900
00069
00070          DO 500 N=1,Z
00071            Y1(N)=-Y1(N)
00072            Y2(N)=-Y2(N)
00073  500    CONTINUE
00074
00075          Q=2
00076          GOTO 100
00077
00078  900    CONTINUE
00079
00080          DO 915 N=1,Z
00081            Y1(N)=-Y1(N)
00082            Y2(N)=-Y2(N)
00083  915    CONTINUE
00084
00085          N=Z
00086
00087            DO 930 I=1,N
00088              W(I,N+1)=-1
00089  930       CONTINUE
00090
00091          CALL GAUSS (N,W)
00092          PRINT*,'      W(I,N+1)','          GAMMA(N)','              LIFT'
00093          PRINT*,'      --------','          --------','              ----'
00094
00095          OPEN (10,FILE='GAMMA.DAT',STATUS='NEW')
00096            DO 950 I=1,N
00097              GAMMA(I)=W(I,N+1)*4*3.1416*Y(I)*OMEGA*ALPHA
00098              L(I)=2*GAMMA(I)*.0023767*Y(I)*OMEGA*(Y2(I)-Y1(I))
00099              PRINT *,W(I,N+1),GAMMA(I),L(I)
00100              WRITE (10,*) Y(I),GAMMA(I)
00101              LIFT=LIFT+L(I)
00102  950       CONTINUE
00103          CLOSE (10)
00104
00105          PRINT*, 'THE TOTAL LIFT IS:',LIFT,'lbs'
00106
```

```
00107     .    OPEN(10,FILE='VLM3.DAT',STATUS='NEW')
00108             DO 960 I=1,N
00109               WRITE(10,*)Y(I),L(I)
00110 960         CONTINUE
00111           CLOSE (10)
00112           END

NUMBER OF WARNINGS IN PROGRAM UNIT: 0
NUMBER OF ERRORS   IN PROGRAM UNIT: 0

00113           SUBROUTINE GAUSS(N,W)
00114           REAL  EPS,EPS2,DET,TM,R,VA,TEMP
00115           INTEGER PV
00116           REAL W(20,21)
00117           EPS=1.0
00118 10        IF (1.0+EPS.GT.1.0)THEN
00119                EPS=EPS/2
00120                GO TO 10
00121           ENDIF
00122           EPS=EPS*2
00123           PRINT*,'MACHINE EPSILON=',EPS
00124           EPS2=EPS*2
00125           DET=1
00126           DO 1010 I=1,N-1
00127              PV=I
00128              DO 20 J=I+1,N
00129                 IF (ABS(W(PV,I)) .LT. ABS(W(J,I)))  PV=J
00130 20           CONTINUE
00131              IF (PV.EQ.I) GOTO 1050
00132              DO 30 JC=1,N+1
00133                 TM=W(I,JC)
00134                 W(I,JC)=W(PV,JC)
00135                 W(PV,JC)=TM
00136 30           CONTINUE
00137 1045         DET=DET*(-1)
00138 1050         IF (W(I,I).EQ.0)GO TO 1200
00139              DO 1060 JR=I+1,N
00140                 IF (W(JR,I).NE.0) THEN
00141                    R=W(JR,I)/W(I,I)
00142                    DO 40 KC=I+1,N+1
00143                       TEMP=W(JR,KC)
00144                       W(JR,KC)=W(JR,KC)-R*W(I,KC)
00145                       IF (ABS(W(JR,KC)).LT.EPS2*TEMP) W(JR,KC)=0.0
00146 40                  CONTINUE
00147                  END IF
00148 1060         CONTINUE
00149 1010         CONTINUE
00150           DO 1070 I=1,N
00151              DET=DET*W(I,I)
00152 1070      CONTINUE
00153
00154           IF (W(N,N).EQ.0) GO TO 1200
00155           W(N,N+1)=W(N,N+1)/W(N,N)
```

```
00156          DO 1080 NV=N-1,1,-1
00157             VA=W(NV,N+1)
00158             DO 1075 K=NV+1,N
00159                VA=VA-W(NV,K)*W(K,N+1)
00160
00161 1075        CONTINUE
00162             W(NV,N+1)=VA/W(NV,NV)
00163 1080     CONTINUE
00164
00165          RETURN
00166 1200     PRINT*,'MATRIX IS SINGULAR'
00167          STOP
00168          END
```

APPENDIX G: MYLAR INFORMATION

MYLAR® POLYESTER FILM

TECHNICAL INFORMATION

PHYSICAL-THERMAL PROPERTIES

ON A ROLL WITH QUALITY

MYLAR polyester film retains good physical properties over a wide temperature range (−70°C to +150°C); and it is also used at temperatures from −250°C to +200°C when the physical requirements are not as demanding. Some physical and thermal properties of MYLAR are summarized in Table 1. Detailed information and other physical and thermal properties are described in the remaining pages of this bulletin.

TABLE I

TYPICAL PHYSICAL AND THERMAL PROPERTIES OF **MYLAR** POLYESTER FILM

PROPERTY		TYPICAL VALUE		UNIT OF MEASURE	TEST METHOD
Gage and Type End Use		92A Industrial	57VB Video Tape		
Ultimate Tensile Strength	MD	26000	29100	psi	ASTM D 882
	TD	31000	33700	psi	ASTM D 882
Strength at 5% Elongation (F-5)	MD	15200	15200	psi	ASTM D 882
	TD	14700	13800	psi	ASTM D 882
Modulus	MD	527000	504000	psi	ASTM D 882
	TD	548000	517000	psi	ASTM D 882
Elongation	MD	106	90	%	ASTM D 882
	TD	84	76	%	ASTM D 882
Surface Roughness Talysurf Ra		0.047	0.031	microns	duPont test
Density		1.392	1.391	grams/cc	ASTM D 1505
Viscosity		0.56	0.56		ASTM D 2857
Melt Point		253	252	°C	DSC*
Dimensional Stability at 105°C	MD	0.5	0.5	%	duPont test
	TD	0.5	0.5		duPont test
at 150°C	MD	1.5	1.8		duPont test
	TD	1.5	1.8		duPont test
Specific Heat		0.28	0.28	cal/gm/°C	
Coefficients of Thermal Expansion		1.0×10^{-5}	1.7×10^{-5}	in/in/°C	ASTM D 696 30-50°C
Thermal Conductivity (MYLAR 1000A)		3.7×10^{-4}	3.7×10^{-4}	$\frac{\text{cal-cm}}{\text{sqcm-sec-°C}}$	25-75°C
UL94 Flame Class		94VTM-2	94VTM-2	Slow to self-extinguishing	

APPENDIX H: HPH DRAWINGS

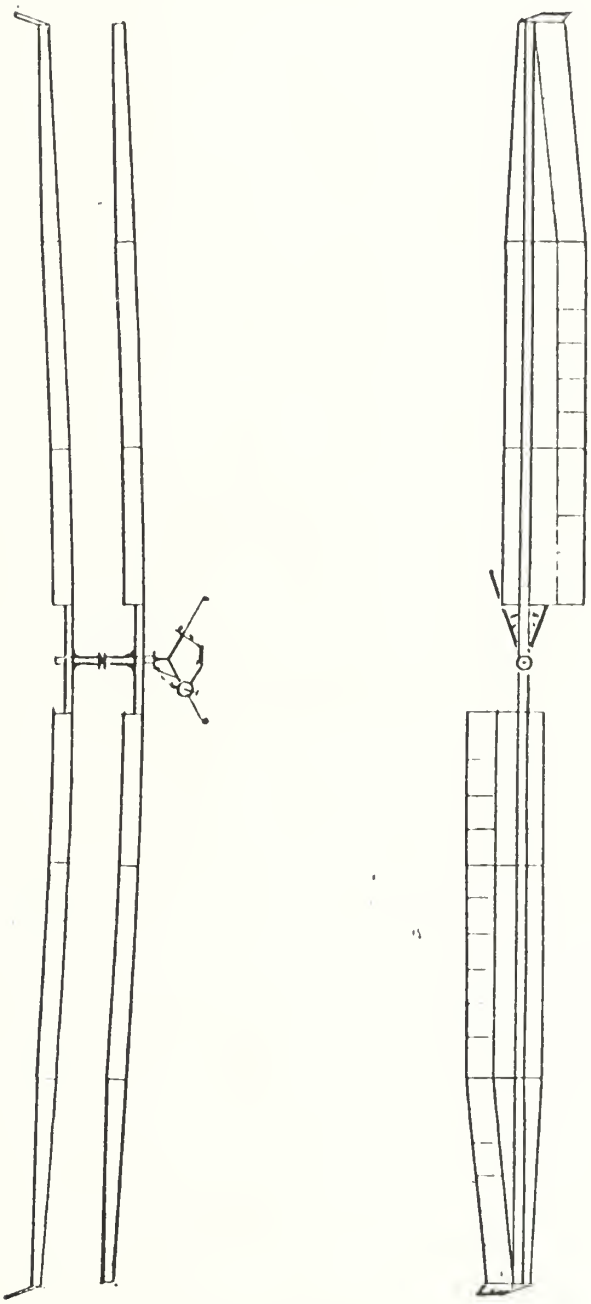

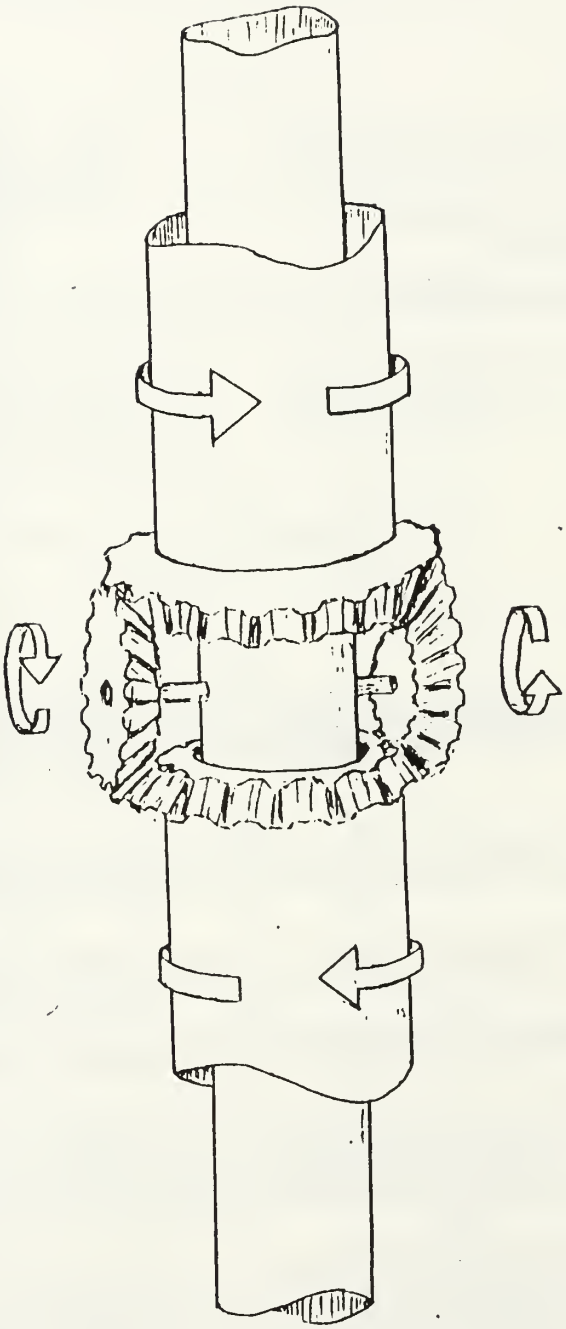

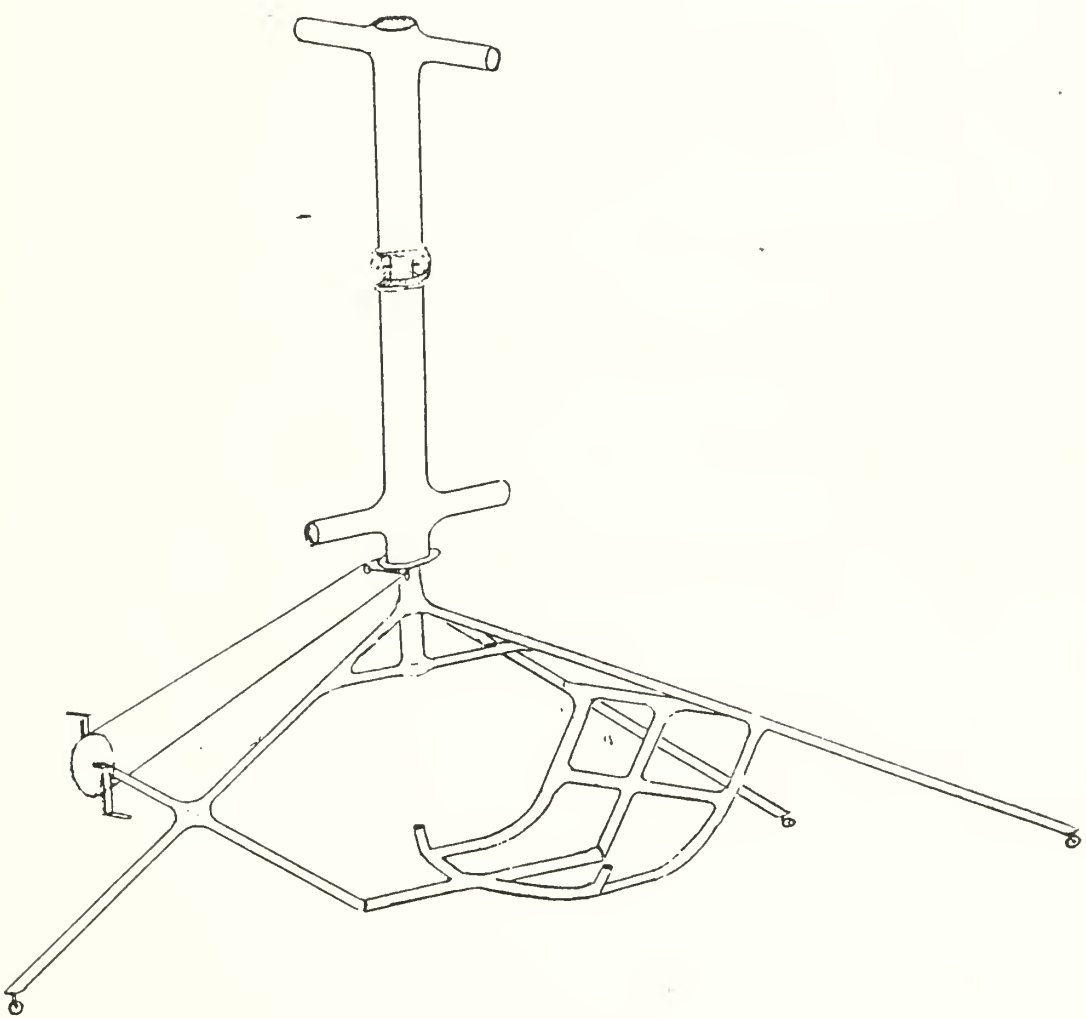

INITIAL DISTRIBUTION LIST

1.	Defense Technical Information Center Cameron Station Alexandria, Va 22304-6145	2
2.	Library, Code 0142 Naval Postgraduate School Monterey, Ca 93943-5000	2
3.	Chairman, Dept. Aeronautics and Astronautics Naval Postgraduate School Monterey, Ca 93943-5000	1
4.	Prof R.M. Howard Code 31 Naval Postgraduate School Monterey, Ca 93943-5000	1
5.	Prof E.R. Wood Code 31 Naval Postgraduate School Monterey, Ca 93943-5000	1
6.	Mr. D.E. Blish PEMCO AEROPLEX P.O.Box 929 Dothan, Al 36302	1
7.	Mr. P. Zwann 225 Churchill Rd. Sierra Madre, Ca 91024	1
8.	Lcdr. S.A. Bruce P.O. Box 179 Valley Lee, Md 20692	1

Thesis
B8255 Bruce
c.1 Human-powered heli-
copter.

Thesis
B8255 Bruce
c.1 Human-powered heli-
copter.

DUDLEY KNOX LIBRARY
3 2768 00016176 4